INKJET PRINTING OF SMART HYDROGELS AND THEIR RESPONSE

CHARACTERIZATION

by

Vishal Bhola

A dissertation submitted to the faculty of
The University of Utah
in partial fulfillment of the requirements for the degree of

Master of Science

Department of Electrical and Computer Engineering

The University of Utah

May 2015

The University of Utah Graduate School

STATEMENT OF THESIS APPROVAL

The thesis of **Vishal Bhola**

has been approved by the following supervisory committee members:

Prashant Tathireddy	, Chair	**Oct 29, 2014** Date Approved
Florian Solzbacher	, Member	**Oct 29, 2014** Date Approved
Jules Magda	, Member	**Oct 29, 2014** Date Approved
Loren Rieth	, Member	**Oct 29, 2014** Date Approved

and by **Gianluca Lazzi** , Chair/Dean of

the Department/College/School of **Electrical and Computer Engineering**

and by David B. Kieda, Dean of The Graduate School.

ABSTRACT

Hydrogels find extensive applications in biomedical research, process control in bioreactors, and metabolite monitoring in human/animal research. However, for commercial success of hydrogel-based products, there needs to be an easy technique or process to dispense pre-polymerized hydrogel in a precise location, in precise microliter volumes. Moreover, the process should be inexpensive and repeatable. Microliters dispensing allows the fabrication of thinner hydrogel structures with large surface area to volume ratio, which translates to faster response times. There exists no technique at present that can produce these hydrogels with microscale precision commercially for these applications. In this project, we use the inkjet printing process for inexpensive, highly repeatable microscale patterning for synthesis of smart hydrogel arrays for various applications with a potential for commercial-scale synthesis.

An Epson Artisan 50 inkjet printer printhead was employed for dispensing pregel solution that essentially comprises the monomer mixture and the initiators required for polymerization. We characterized this printer for the resultant size of the synthesized hydrogels under various conditions. The effect of oxygen plasma treatment duration on contact angle of water-glass substrate was obtained to control the spread of the pregel and height of the hydrogels. Magnetic field variation was chosen as the preferred transduction mechanism to translate the hydrogel swelling and deswelling. For this, the hydrogel sensors were equipped with either a magnetic sheet or embedded magnetic particles as the source

of magnetic field. A set of COMSOL simulations were performed to understand the effect of particle density and magnetization of the magnetic particles and sheet on the magnetic field variation. The synthesized magnetic hydrogel sensors were characterized for their response time to varying analytes concentrations. Response times (τ_{90}) of 6 minutes and 15 minutes were obtained for hydrogel sensors with magnetic sheet and magnetic particles, respectively.

TABLE OF CONTENTS

LIST OF TABLES

LIST OF FIGURES

ACKNOWLEDGEMENTS

This project has been an interesting and challenging experience. I feel blessed to have many talented and helpful people around me, whose cooperation, input, and support have helped me extremely to realize the project objectives. First of all, I am extremely grateful to Dr. Prashant Tathireddy for believing in me and providing me with such an excellent opportunity to work on this project. Besides his constant guidance and support, I really appreciate the confidence and freedom vested in me to explore various ideas during the course of this project.

I thank Dr. Jules Magda and Dr. Loren Rieth whose constant input, suggestions, and intriguing questions have always been instrumental in motivating me to be a better researcher. I would like to thank Dr. Florian Solzbacher for his inputs on understanding the theoretical side of the project and simulations. I am extremely grateful to Seung Hei Cho for helping me with the experimental procedures and chemistry side of the project. I would like to thank Rohit Sharma for his help in preparing the magnetometer and other laboratory trainings. Next, I wish to thank my wonderful parents, brother, and sister. Their constant encouragement and support to go live my dreams has been instrumental in inspiring me to pursue my master's degree. I am extremely grateful for their love and constant belief in me. Finally, I thank my friends Anurag Upadhyay and Atul Sancheti, who have always been by my side in both good and bad times, believed in me, and provided their honest feedback.

1. INTRODUCTION

1.1. Hydrogels

Hydrogels can be described as networks of polymers both natural and synthetic, which can potentially absorb up to thousands of times their dry weight in water. The ability to hold an enormously large volume of water basically arises from the presence of hydrophilic groups such as –OH, –COOH, –SO3H etc. present on the polymeric chains forming the networks. Hydrogels can be made to be chemically stable or degradable with time. On the basis of preparation, hydrogels can be broadly classified as physical and chemical hydrogels [1-3].

1.1.1. Physical or Reversible Hydrogels

In physical hydrogels, the polymeric networks are held together by molecular entanglements and/or secondary forces, including ionic, hydrogen bonding, or hydrophobic forces. Because of the inconsistency in these forces across the networks as well as the free chain ends loops, these hydrogels are typically nonhomogenous. An example of physical hydrogel is shown in Figure 1.1 (a) where the alginate chains are held via interactions arising at the Ca^{2+} junctions [3].

1.1.2. Chemical or Permanent Hydrogels

Chemical hydrogels are covalently cross-linked polymeric networks and are produced by copolymerization of monomers, cross-linking of water soluble polymers, or altering the hydrophobic polymers making them hydrophilic and subsequent cross-linking to produce networks. Chemical hydrogels are also nonhomogenous networks which arise due to the aggregation of hydrophobic cross-linking agents, phase separation during the polymerization, or free chain ends and loops. Figure 1.1 (b) shows an example of chemical hydrogel where the acrylamide chains are cross-linked by BIS [3]. Presented research also employs chemically cross-linked hydrogels with yes poly-acrylamide backbone with a different chemical composition that will be described in later chapters.

1.2. Applications of Hydrogels

Hydrogels are characterized as being naturally soft, elastic, and hydrophilic, which makes them an excellent resource in engineering advanced material design. Besides the
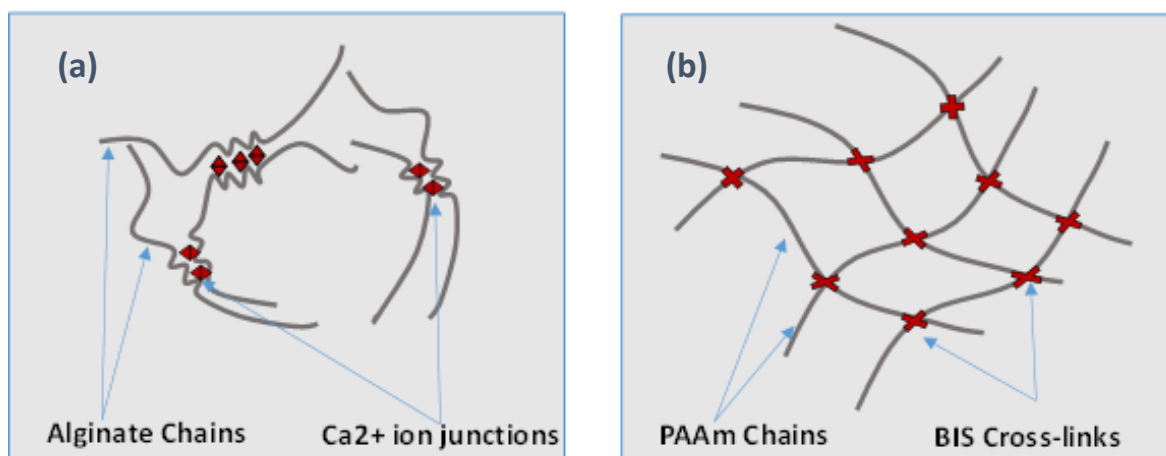
Figure 1.1: Examples of (a) physically cross-linked hydrogel and (b) chemically cross-linked hydrogel. Adapted from [3]

extensive functional groups present on the polymeric networks, additional functional elements can be incorporated in the hydrogel matrix, thus making them useful for specific tasks. Hydrogels can be made to be biodegradable, which lends its applications in tissue engineering [4]. Moreover, because of their biocompatibility, ease, and wide range of synthesis techniques as well as ability to be fabricated at multiple size scales, hydrogels have been of great interest in extensive applications ranging from diagnostic tools, environmental applications as well as biomedical applications like contact lenses [7] and drug delivery [5, 6]. Hydrogels tailored chemically for detection of different analytes, e.g., glucose sensing, CO_2 sensing, etc. as well as environment sensitive, e.g., pH sensitive, heat sensitive, etc. have also been synthesized. This opens up a myriad set of potential applications for hydrogels, e.g., in building medical sensing devices, sensors in bioreactors, water management plants, etc. [8]. These applications are summarized in Figure 1.2.

1.3. Limitations of Present Synthesis Methods

Hydrogels have been synthesized in sizes ranging from nanoscale particles to macro-scale forms. Most of the approaches involve synthesizing the hydrogel and then transferring them postsynthesis. However, hydrogels are typically mechanically weak and difficult to handle. So transferring the hydrogels postsynthesis is difficult and can lead to breakage or/and integration issues with the transduction setup. This limits the potential application of hydrogel sensors, especially when their alignment is integral to proper transduction. An example of this is the magnetic transduction system employed in the presented research. The change in swelling of the magnetic hydrogel sensor in response to varying analyte concentration is transformed to a change in the magnetic field strength

Tissue engineering [4]

cartilage defect   gel filled defect

Biomedical devices [7]

Bioprocess control [8]

Drug delivery applications[5, 6]
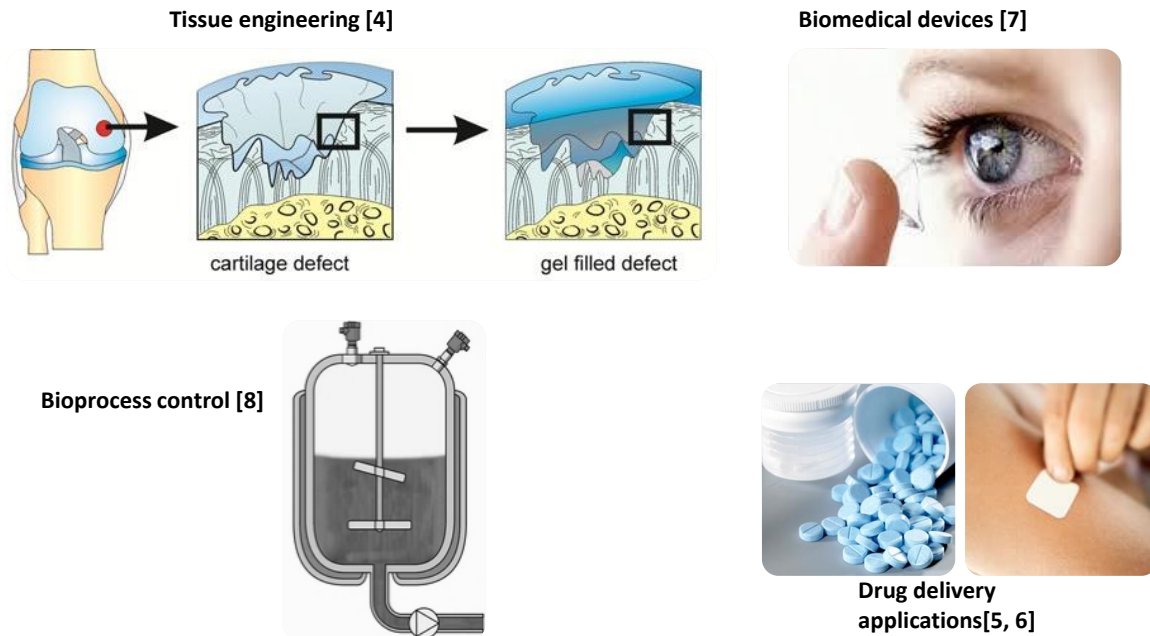
Figure 1.2: Applications of hydrogels in various areas like tissue engineering, bioprocess control, drug delivery, and biomedical devices.

which is then read by the magnetometer and transmitted over a ZigBee link to the receiver for further processing. This requires for the source of magnetic field (embedded magnetic particles inside the hydrogel or magnetic sheet attached to it) to be aligned accurately with the magnetometer, which is however difficult to achieve post the hydrogel synthesis. Moreover, for commercial success of hydrogel-based products and applications, there needs to be an easy repeatable technique or process to synthesize hydrogels in precise location, in precise microliter volumes.

Also, for applications such as real-time monitoring of analytes in bioreactors and continuous glucose monitoring in diabetic patients, it becomes imperative to synthesize sensors with fast response times. It has been shown earlier that the hydrogel sensor's response time decreases with decrease in the hydrogel size. Figure 1.3 presents a graph of response time and magnitude versus the hydrogel thickness for a pH sensitive hydrogel [8].
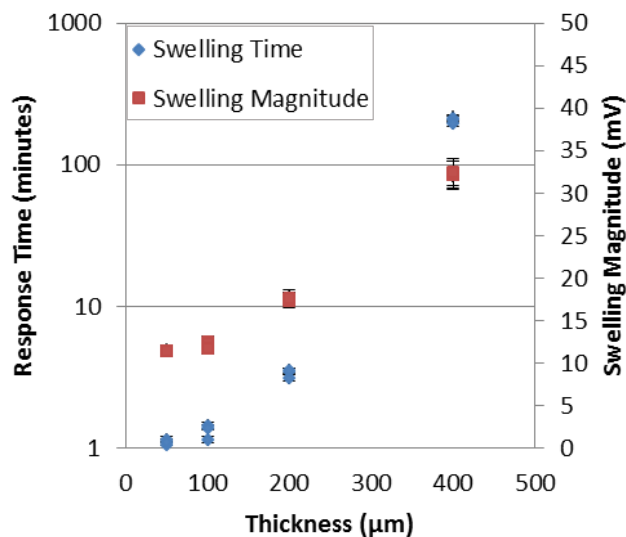
Figure 1.3: Response time and magnitude versus hydrogel thickness for a pH change between 7.2 and 7.4 in PBS buffer.

Spin-coating and emulsion polymerization techniques are two potential approaches for synthesis of thin hydrogel structures with thickness in a few hundred nanometers to micrometers. Besides being expensive, spin coating does not allow accurate control of the shape of the synthesized structures and as with macro-gels, the handling of these ultra-fine hydrogels is even more difficult. Emulsion polymerization techniques, on the other hand, can be used to synthesize hydrogels in the shape of beads. Again, it suffers from patterning and handling issues as well as integration issues with the transduction setup.

1.4. Inkjet Printing

Inkjet printing is a digital deposition method that offers the ability to directly deposit picoliters of solutions or suspensions in user-defined patterns. Inkjet printing is highly accurate, non-contact, and offers high resolutions. This ability has led to the use of inkjet printing to evolve as an important technology in applications like flexible electronics, tissue

engineering, and MEMS devices. The ability to dispense the solutions accurately in exact locations allows maskless patterning, thereby making it an inexpensive yet efficient alternative to MEMS fabrication techniques like lithography and spin coating etc. Moreover, the non-contact dispensing technique helps prevent contamination issues [9-11]. Inkjet printers can be broadly classified as drop-on-demand and continuous printers [12]. A more detailed classification of the inkjet printers is presented in Figure 1.4.

1.4.1. Continuous Inkjet (CIJ)

CIJ printers eject drops continuously at high frequencies (50 kHz to 175 kHz) which are charged with an electrostatic field and deflected to control their position on the substrate. CIJ printers collect the unprinted drops for reuse. CIJ printing offers high speed because of the high-frequency droplet ejection.
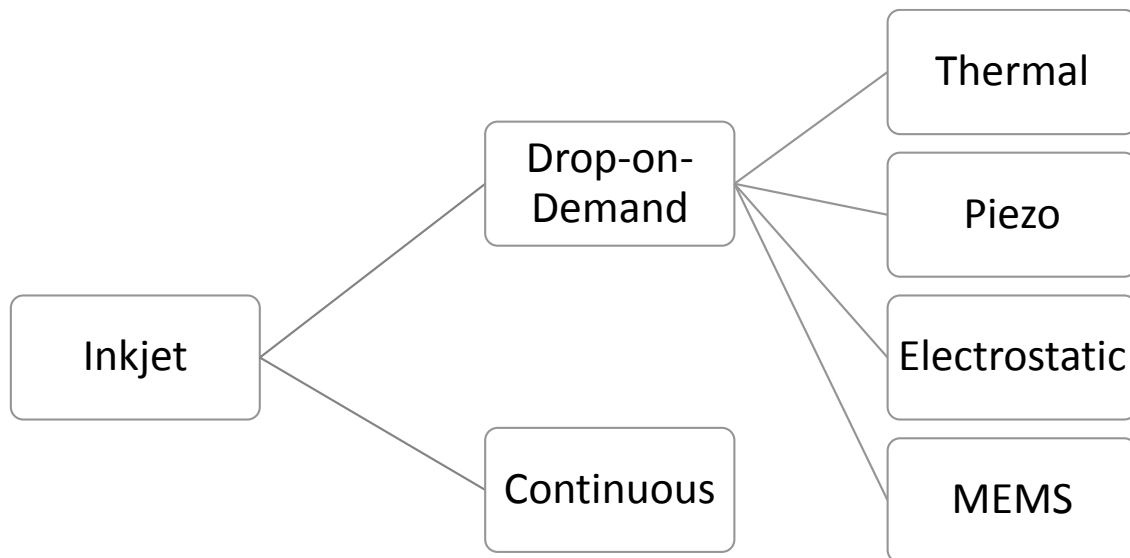
Figure 1.4: Classification of Inkjet printers.

1.4.2. Drop-on-demand Inkjet (DOD)

Drop-on-demand printers use pressure pulses to dispense ink drops only when required. These pressure pulses can be generated using various methods like thermal, piezoelectric, and electrostatic [12]. Thermal DOD printers work by heating up a resistive element up to 400 °C which vaporizes the ink creating a bubble which in effect produces the pressure pulse and forces the ink droplet out of the nozzle.

Though thermal printers offer the potential for smaller drop sizes and lower cost, they are inherently limited by the fluids that can be used because they must be vaporizable besides withstanding such high temperatures. Piezoelectric DOD printers use mechanical vibrations to deposit precise volumes of the ink and hence offer the feasibility to deposit a wider range of materials as compared to the thermal printers which heat up the ink [9]. The working principle of a piezoelectric DOD printer is presented in Figure 1.5.

Inkjet printing has also been applied to print hydrogels [13-16]; however, there is not enough scientific data to the best of our knowledge as to the printing of composite magnetic hydrogels with embedded magnetic particles. In this project, we propose the use of inkjet printing process for inexpensive, highly repeatable microscale patterning for synthesis of smart hydrogel arrays for various applications with a potential for commercial-scale synthesis.

1.5. Project Goals and Objectives

The goal of this project was to provide proof of concept for the implementation of smart hydrogels with embedded magnetic particles using inkjet printing and to characterize the response of these printed hydrogels for different analytes. Specific objectives to achieve
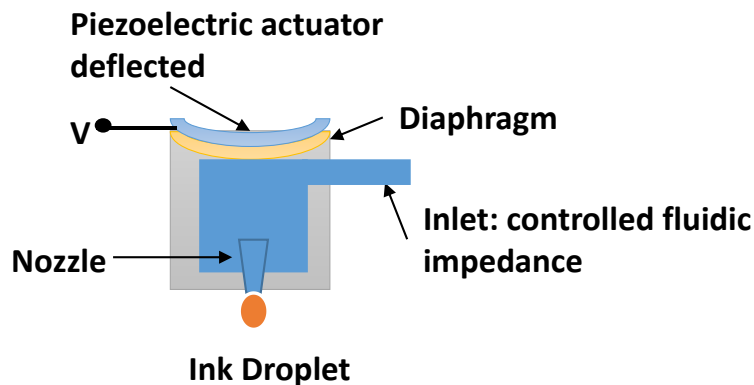
Figure 1.5: Working principle of piezo inkjet printer. The deflections in the piezoelectric actuator corresponding to the digital signal from the computer, force the ink droplets to be ejected from the cartridge onto the substrate.

the goal are presented next.

1.5.1. Printer Characterization

Description: Here we characterize the printer to determine the following:

i.   Minimum number of printed layers to achieve a single continuous layer of the pregel solution on different substrates

ii. Thickness of the printed hydrogel versus the number of printed layers

iii. Variability in the height of the printed hydrogels across different samples

Motivation: This aim will help determine the repeatability of the printing process and define the precision and accuracy of the process as a potential commercial synthesis method. Factors influencing this aim are mostly the hydrophilicity of the substrate which will be studied in the next aim.

Anticipated results: Printer characterization results in the form of graphs and statistical measures for better understanding and design of the process.

1.5.2. Substrate Treatment and Its Effect on Surface Hydrophilicity

Description: In this aim, we will test the effect of oxygen plasma activation of the glass substrate to determine the hydrophilicity of the surface and optimal duration for plasma activation will be obtained. Also, GelBond® film will be used to compare the spread with plasma activated glass substrate.

Motivation: This aim will help understand the spreading of the pregel solution on the substrate's surface. This is an important step because surface hydrophilicity determines the shape and height of the pregel solution and hence the polymerized hydrogel. The comparison with GelBond® film will help determine the right substrata for intended application of the synthesized hydrogels.

Anticipated results: The hydrophilicity of the substrate's surface will be interpreted using the contact angle measurements using the data obtained from Zygo optical interferometer. Deviation in shape/size from the expected size will be presented using statistical measures.

1.5.3. Printing Composite Hydrogels with Embedded Magnetic Particles

Description: This aim will test the feasibility of inkjet printing the pregel solution with dispersed magnetic particles to synthesize the composite hydrogels. Further, as in aim 1, this step will characterize the effect of dispersed particles on the printed hydrogels' size, shape, etc.

Motivation: Inkjet printers can easily dispense liquid inks as far as their physical properties are within the specified limits. However, there is no prior scientific data to the best of our knowledge on printing of inks/solutions with magnetic particles.

Anticipated results: Feasibility analysis for printing pregel solution with dispersed

magnetic particles and composite hydrogels of varying thickness and size.

1.5.4. Theoretical Simulations

Description: This aim will explore the use of COMSOL simulations for the magnetic hydrogels by constructing models similar to the synthesized hydrogel sensors and observing the spatial magnetic field variation. Simulations will be performed for two implementations of the hydrogel sensors 1) hydrogel with magnetic sheet on top and 2) hydrogel with embedded magnetic particles. For the latter implementation, the effect of particle size and density will also be studied.

Motivation: Theoretical simulations will help achieve better understanding of the magnetic field variation around the sensor and provide guidelines to select the right particle size and density. This will also enable better design of the experiments to characterize the synthesized hydrogel sensors.

Anticipated results: Magnetic field variation plots for magnetic sheet and magnetic particles of varying sizes and density.

1.5.5. Response Characterization of Hydrogels

Description: This aim will characterize magnetic hydrogels by correlating the changes in magnetic field to changes in analytes concentrations. Different alignment configurations of the magnetic particles inside the hydrogel will be used to identify the optimal configuration.

Motivation: Within this aim, we will conduct experiments to thoroughly characterize changes in magnetic field intensity to changes in analytes concentration using the magnetic

hydrogels developed in aim 3. The results will help optimize the hydrogel chemistry and magnetic particle concentration.

Anticipated results: Characterization results for a range of analytes (glucose, ionic strength, pH, etc.) by varying their concentration in media solution.

2. INKJET PRINTING AS THE PRESENTED SOLUTION

Here, we present a process for inexpensive, highly repeatable microscale patterning for synthesis of smart hydrogel arrays for various applications with a potential for commercial-scale synthesis. As described earlier, position control and volume control are the two most important things for achieving repeatable commercial-scale hydrogel synthesis. Modern inkjet printers can dispense as low as 1.5 picoliters per drop with resolutions up to 5760 x 1440 dpi and thus can help achieve these two tasks quite efficiently with little or no modification in the printer setup. Therefore, we present the use of inkjet printing to dispense accurate volumes of the pregel solution and subsequent polymerization of the dispensed solutions to synthesize fine hydrogels and hydrogel arrays. Figure 2.1 highlights the implementation flow for the presented process. The implementation steps are described next.

Tailor pre-polymer properties
- Pre-polymer solution chemistry
- Pre-polymer solution fluidic properties
- Particles size, dispersion

Substrate Treatment
- Substrate Selection
- Cleaning
- Improve hydrophilicity

Inkjet Printing
- Pattern using software
- Number of layers

Polymerization
- UV Curing
- Thermal Curing

Align Particles
- Magnetization
- Alignment
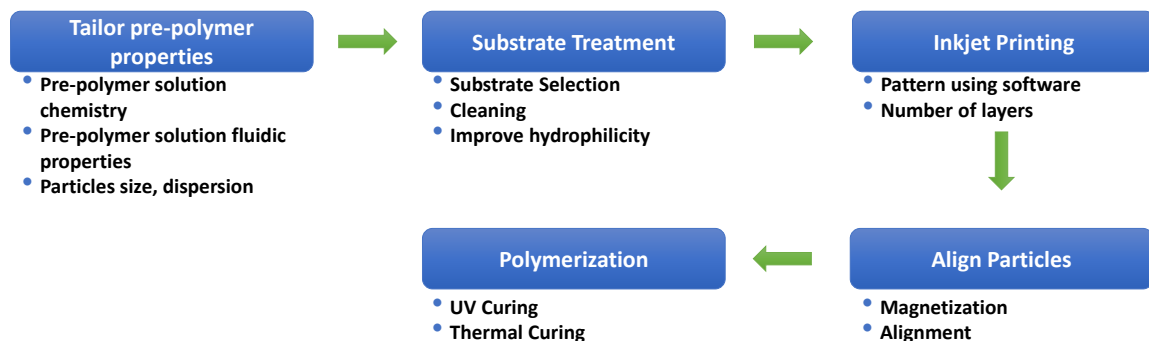
Figure 2.1: Implementation block diagram for the proposed solution.

2.1. <u>Tailor the Properties of Pregel Solution</u>

The first step deals with the tailoring of the chemical properties of the pregel solutions to render them sensitive to particular analytes and then to alter their fluidic properties like viscosity, surface tension, etc. and make it compatible to be dispensed through fine nozzles with diameters in the range 10 μm- 100 μm used typically in modern inkjet printers.

Engineering of fluidic properties of pregels can be done by adjusting the composition of ingredients in pregel while still retaining the chemical properties of the polymer or/and adding viscous liquids/surfactants like Triton X, sodium oleate, etc. while still maintaining the molar ratio of the constituents. Altering these fluidic properties also enables the use of commercial inkjet printers for synthesis of hydrogel structures with little or no modification of the printer.

Conventional ink chemistry is fairly complex requiring a number of components [17] (Figure 2.2) to serve different ink requirements. However, every ink needs to satisfy certain fluidic properties for it to be dispensable through the nozzles. These properties and their ranges are highlighted in Table 2.1 [10, 11].
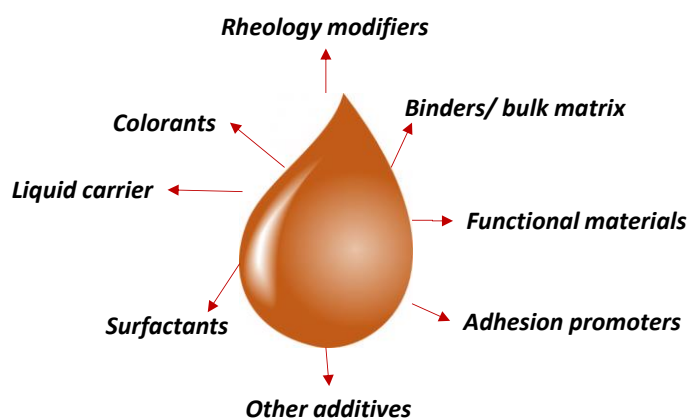
Figure 2.2: Components of a typical inkjet ink (adapted from [17]).

Table 2.1: Desirable fluidic properties for inkjet printing.

Viscosity (piezo)	8- 15 cP
Viscosity (thermal)	< 3 cP
Surface Tension	25 – 35 dyne/cm

We then disperse specific particles into the pregel solution. This involves tailoring the particle sizes to different nozzle sizes allowing easy dispersion from the nozzle heads. Another important part of this step is to decide the nature and size of the particles that will be dispersed in the pregel solution, to enable the transduction of the change in the size of the hydrogels in response to different analytes. This is basically derived from two important considerations.

1) Signal transduction mechanism to be used

Pressure sensors have been used extensively for transducing the swelling/deswelling of the hydrogel in response to pH, ionic strength, etc. [18-20]. However, they are expensive and offer limited capabilities for integration in a wireless setup. In this project, we will be exploring the use of magnetic particles and change of magnetic field strength with varying hydrogel thickness as the preferred mechanism for signal transduction.

2) The size of the nozzles in the printhead

In general, it is preferred to have the size of the particles selected to be less than 1/10th of the nozzle diameter. However, if the size of the particles is less than their Critical Diameter [21], the magnetic nature of the particles changes and it most likely will alter the signal transduction mechanism. Table 2.2 highlights the particle sizes required for the corresponding nozzle diameter to enable easy dispersion.

Table 2.2: Particle sizes for different nozzle diameters.

Nozzle Diameter	Particle size range
5- 10 μm	50 nm – 0.1 μm
10 – 20 μm	50 nm – 0.2 μm
20 – 50 μm	50 nm – 1 μm

2.2. Substrate Selection/Treatment

The next step deals with the selection and surface treatment of the right substrate for printing the hydrogels. Liquid drop size on the substrate is strongly dependent on contact angle θ [10]. For a given dispensed volume, the size of the droplet is given by the relation:

$$Volume = \frac{\pi}{3} * r^3 * [\frac{2 - 3 * cos\theta + cos^3\theta}{4 * sin^3 \theta}]$$

where, θ is the contact angle and r is the radius of the drop.

Therefore, surface treatment is necessary to control the substrate's hydrophilicity, which in turn controls the spread and height of the dispensed solution. This becomes more important when we are trying to print the hydrogels in specific shapes and sizes.

Substrates that will be explored in the proposed project include glass and GelBond® acrylamide film. GelBond® film has a layer of acrylamide on the surface that bonds chemically with the hydrogel upon UV curing. The surface is hydrophilic and needs no surface treatment except surface cleansing. Untreated glass, however, has a high contact angle (~50 degrees), This causes problems when printing multiple layers at the same substrate location and more so when printing composite hydrogels because the curve surface profile forces the particles in the composite hydrogel to slide down. The surface

hydrophilicity of glass substrate, however, can be improved significantly with oxygen plasma treatment. Oxygen plasma activates the surface of glass by introducing hydroxyl groups and removing the contaminants present on the glass surface [22, 23]. As a result, the glass surface becomes more hydrophilic and water-glass contact angle is lowered. When printing hydrogels, plasma activation helps establish a weak physical bond between the substrate and the synthesized hydrogels, which reduces the risk of losing the hydrogels in media solution. The contact angle and bond strength are a function of plasma exposure duration [24, 25]. This project will also investigate the effect of duration on contact angle.

2.3. Dispensing the Pregel Solution

The pregel solution with or without the dispersed particles can then be dispensed and patterned through the inkjet printer. In general, specialized printheads like Xaar, MicroDrop Dispenser Heads, etc., can also be used for dispensing [15, 16]. While the inkjet printers can be controlled via proprietary drivers and software, the specialized printheads can be controlled to output the desired volumes and shapes using software on a computer or embedded programs on microcontrollers. By controlling the amount of pregel dispensed through these nozzles and using multiple layers, the size and shape morphology of the fabricated structures can be controlled with micrometer precision.

2.4. Magnetization and Alignment of Particles Inside the Hydrogels

The particles may be premagnetized prior to dispersion inside the pregel solution. However, the individual magnetic moments of these particles may be oriented in different directions inside the printed hydrogel. This results in a low net magnetic moment for the

composite hydrogel sensors. Therefore, in this step, the particles inside the printed pregel solution are aligned by application of external magnetic field to intensify the signal transduction corresponding to the physical changes in the hydrogels when sensing the analytes. In the other case, when the particles were not premagnetized before printing, application of external magnetic field would magnetize the particles and align them in the same direction to give a strong net magnetic moment to the hydrogel sensor. The magnetization can be achieved by using strong bar magnets or by using electromagnetic coils. Having these external magnets oriented in different configurations, the particles can be aligned vertically or horizontally or in a halbach array fashion with strong magnetic field only on one side of the hydrogel.

2.5. Polymerization

Lastly, the polymerization is carried out using either UV curing or thermal curing. Curing parameters like light intensity, duration of exposure, etc. need to be set to achieve the desired hydrogel properties. Also, as an alternative to magnetizing the particles in the previous step, they can be aligned post the curing process. However, the particles must be homogeneously distributed inside the hydrogel for a strong net magnetic moment. When multiple sandwich hydrogel layers need to be produced on the same substrate area, the dispensing and polymerization steps can be repeated as required. An example synthesis for a two-tiered hydrogel structure, without and with magnetic particles, is highlighted in Figure 2.3.
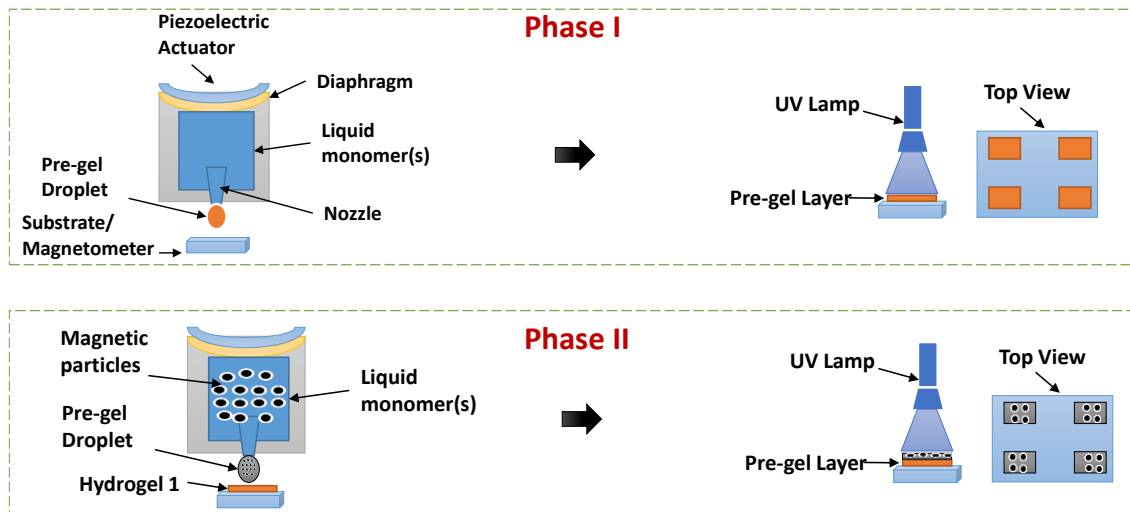
Figure 2.3: Synthesis of a hybrid two-layer hydrogel structure, with the top layer having dispersed magnetic particles.

3. EXPERIMENTS AND RESULTS

3.1. Theoretical Simulations

In order to achieve the best performance using the magnetic signal transduction, it becomes imperative to identify the optimum parameters for the magnetic particles or the magnetic sheet. A set of simulations were performed in COMSOL Multiphysics software to determine the optimum values/ranges for these parameters. COMSOL with MATLAB was used to automate the model construction and simulation. Hydrogel geometry in all the experiments was fixed at: L x W x H = 20 µm × 20 µm × 50 µm, unless otherwise specified. For the simulations with magnetic particles as the source of magnetic field, a double layer hydrogel geometry was employed. This is done to ensure that the simulations are a close approximation of the actual experiments. Only one hydrogel layer was used for the magnetic strip simulation. The hydrogel geometries with distributed particles and magnetic sheet are shown in Figures 3.1 and 3.2 respectively. Specific model construction details for the different simulations performed are described next.

3.1.1. Magnetic Particle Density

Particle density can be specified as the weight or volume percentage with respect to the hydrogel. A low particle density implies lower resulting magnetic field, whereas a high particle density can possibly cause loading of the hydrogel and affect its swelling
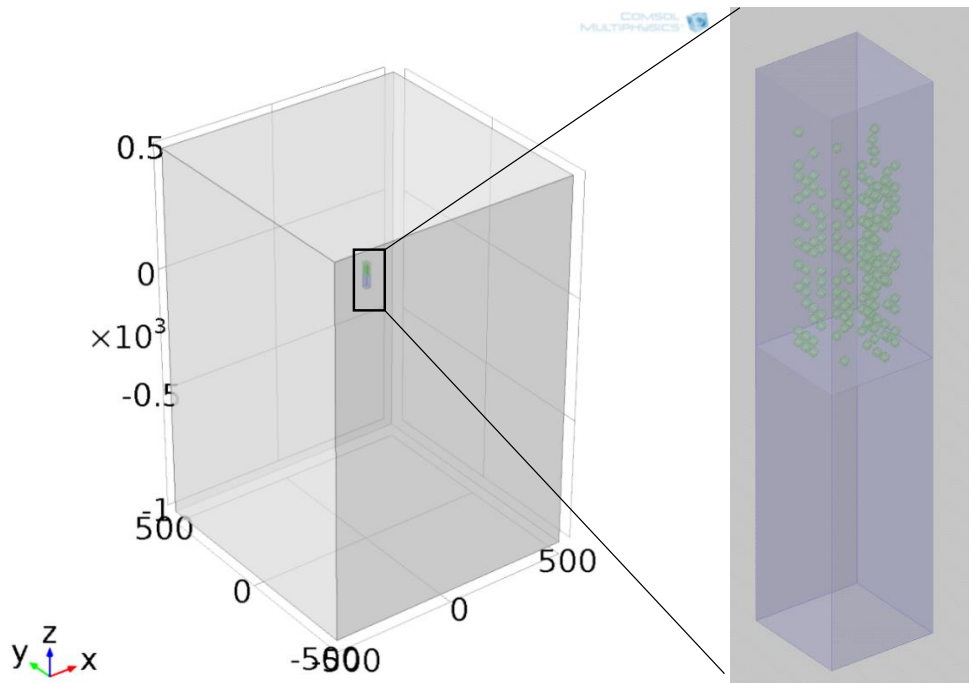
Figure 3.1: COMSOL geometry for double layered hydrogel with uniformly distributed magnetic particles in the second layer.

characteristics, which would basically mean that it is no longer just controlled by the osmotic pressure forces arising due to the imbalance in the concentrations in and out of the hydrogel. The particle density at a given particle size for the simulations was varied from 1% w/w to 20% w/w as the upper limit. The particles were distributed uniformly throughout the hydrogel by using the MATLAB's randi() function to generate a set of integer locations spaced along the axis to accommodate the particles making sure no two particles intersect each other. This becomes essential when the different domains are assigned the materials and properties. If the particles are intersecting, it creates additional domains, which can lead to errors in simulation if unaccounted for or create meshing problems if the size of these intersection regions are below the specified minimum size for meshing different domains.
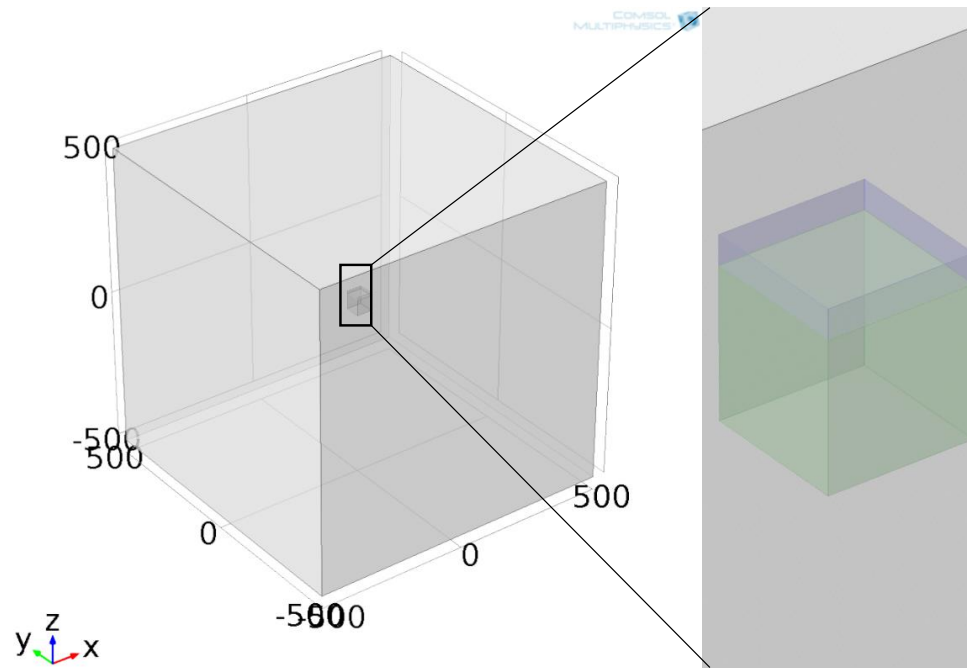
Figure 3.2: COMSOL geometry for single layered hydrogel with magnetic sheet on top.

3.1.2. Particle Size

The remanent magnetization of the magnetic particles typically increases with the size of the particles [26]. However, the inkjet nozzle sizes to be used for printing will impose an upper limit on the size of these particles, as described in Chapter 2. Also, the magnetic particles behave as superparamagnetic below the critical diameter. Therefore, for the given setup design, they must be larger than critical diameter and be smaller than the maximum nozzle size available in the inkjet printers.

3.1.3. Particle Magnetization

The particles must carry a minimum magnetization, which ensures that the magnetic field strength variation from the resulting structure matches the sensitivity of the

magnetometer, for the changes in the hydrogel swelling/de-swelling to be appropriately transformed into changes in signal from the magnetometer.

For the particles synthesized in house as well as the magnetic sheets, the remanent magnetization values were obtained by characterizing the samples using a vibrating sample magnetometer (VSM). Figure 3.3 presents the setup configuration used in the VSM for obtaining the hysteresis curve.

3.1.3.1. Magnetic Particle Characterization

The particles dispersed in water were deposited drop by drop on scotch tape and dried before characterizing them in the VSM. The particles' weight was determined by subtracting the weight of the scotch tape from the weight of particles and scotch tape together. The scotch tape with the deposited particles was cut into appropriate size to affix it on the circular sample holder 8mm in diameter.
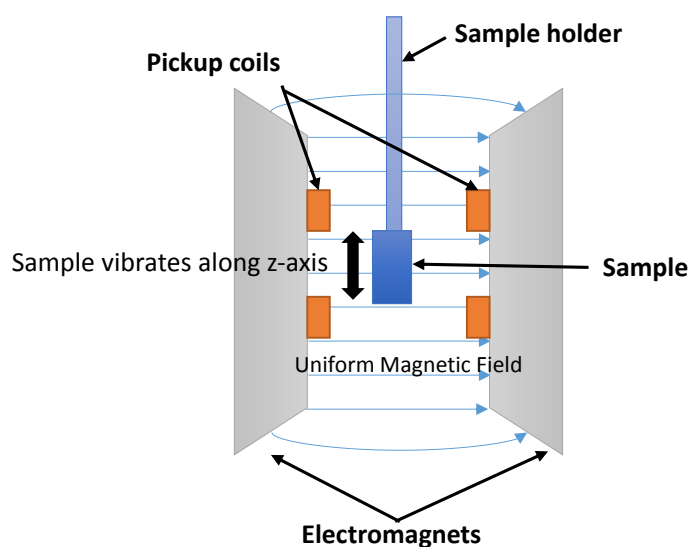
Figure 3.3: Setup configuration used for magnetizing and characterizing the magnetic particles and magnetic sheet samples

3.1.3.2.Magnetic Sheet Characterization

Two sheets of thickness 230 µm and 300 µm were used for the experimentation. 5 mm x 5 mm square samples were cut from the magnetic sheets and placed on the sample holder one by one. Three samples were used for each of the magnetic sheet and their weights are recorded in Table 3.1.

The applied magnetic field in the VSM was varied from 0 T to 1.8 T in a symmetric half loop to obtain the magnetization curve. Further, the magnetization values from the magnetization curve obtained from the VSM were normalized with respect to weight. These normalized magnetization values (in emu/g) are plotted in Figure 3.4 for the magnetic particles. As is evident from the magnetization curve, the remanent magnetization that these particles carry is too small as compared to the saturation magnetization. In other words the particles are close to being superparamagnetic and hence cannot be used in the present transduction mechanism.

Table 3.1: Weights of the magnetic sheet and magnetic particles samples for the VSM characterization experiments.

Magnetic Sheet 1, Thickness: 300 µm	
Sample 1	0.0294 g
Sample 2	0.0296 g
Sample 3	0.0296 g
Magnetic Sheet 2, Thickness: 230 µm	
Sample 1	0.0191 g
Sample 2	0.0192 g
Sample 3	0.0196 g
Magnetic Nanoparticles (Synthesized in-house)	
Sample 1	0.0022 g
Sample 2	0.0020 g
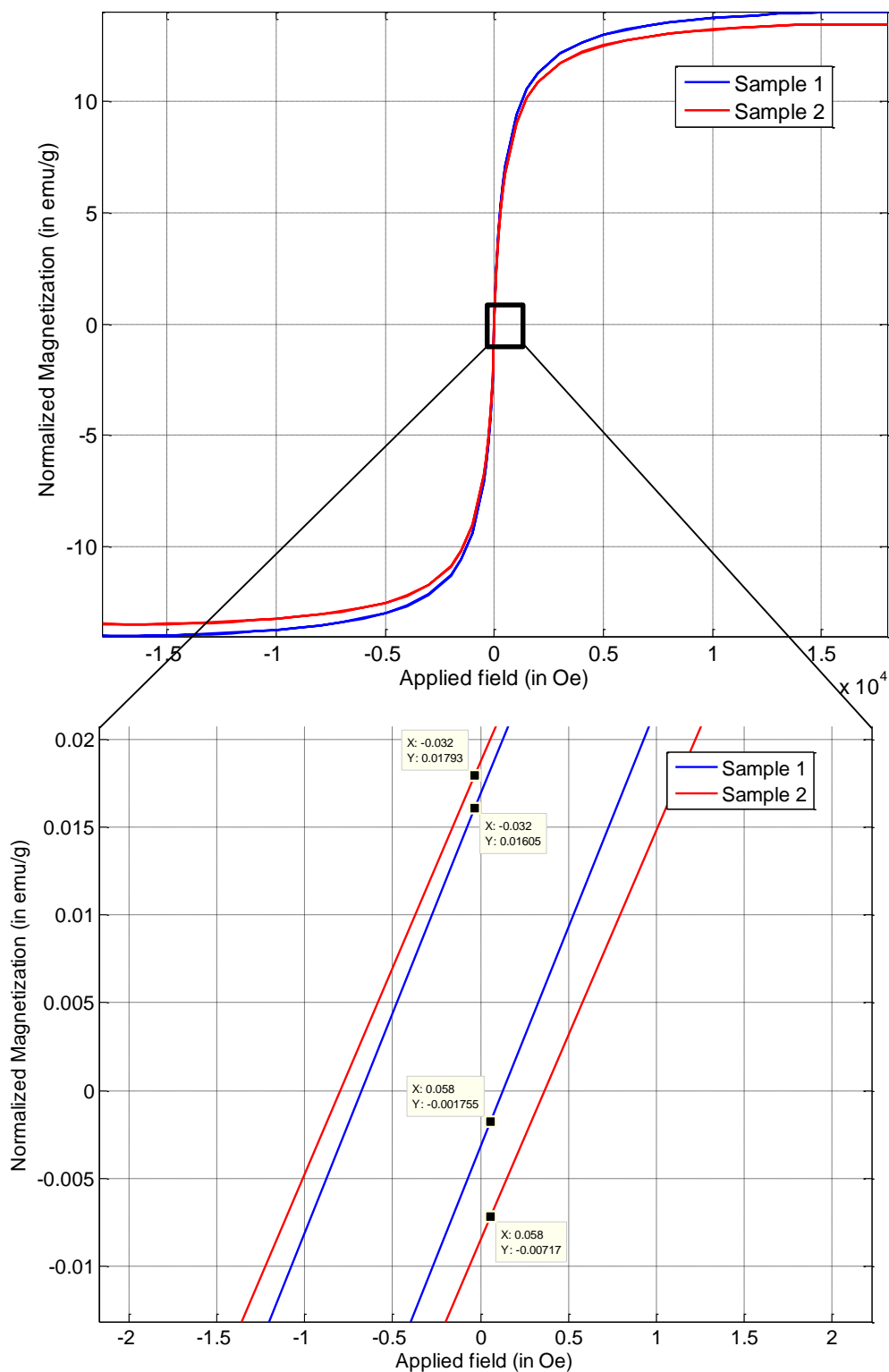
Figure 3.4: Hysteresis loop for the synthesized magnetic particles for applied field strength between -1.8 T and 1.8T. Since the particles have nearly zero coercevity and remanent magnetization, they are superparamagnetic.

Figure 3.5 and 3.6 present the magnetization curves for the magnetic sheets of thickness 300 μm and 230 μm, respectively. The average values obtained for the remanent sheet magnetization at zero applied magnetic field are 27.9 emu/g and 22.4 emu/g, respectively. These sheets were cut into further smaller parts and used for the laboratory experiments to characterize the response of hydrogels to varying ionic strength.

3.1.4. Hydrogel with Magnetic Particle Simulation

COMSOL simulations were performed for the geometry depicted in Figure 3.1, at a set of particle sizes ranging from 1 μm to 3 μm. The particles were uniformly distributed within the hydrogel as described earlier. The particle size determined the minimum mesh size in all the simulations. The magnetic field variation versus the varying distance from
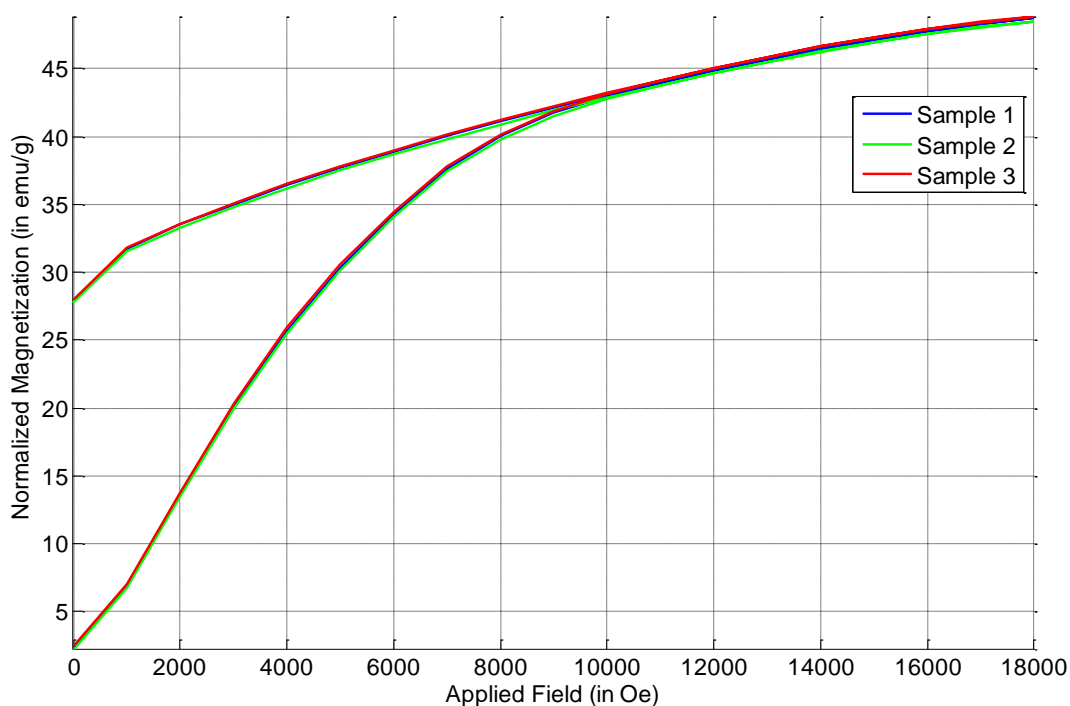
Figure 3.5: Magnetization curve for the magnetic sheet of thickness 300 μm. The sheets carry an average remanent magnetization of 27.9 emu/g.
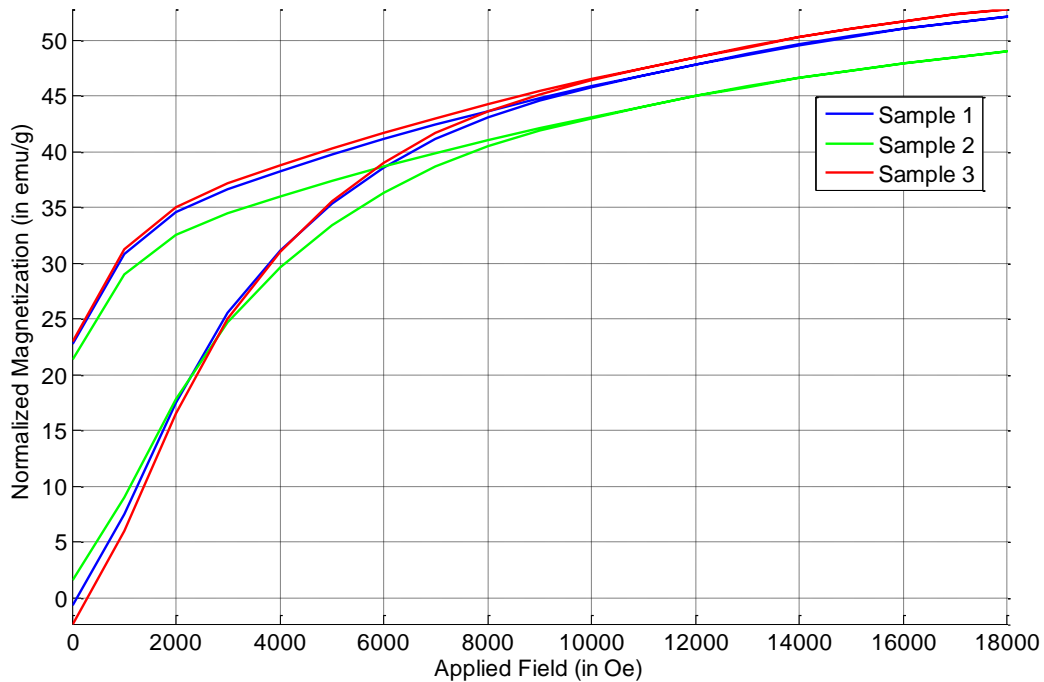
Figure 3.6: Magnetization curve for the magnetic sheet of thickness 230 µm. The sheets carry an average remanent magnetization of 22.4 emu/g.

the hydrogel along the z- direction was obtained for the different particle sizes and density values. The remanent magnetization for the particles varies with the size of the particles but was kept constant at 27.9 emu/g, which was the remanent magnetization value obtained for the magnetic sheet of thickness 300 µm. Table 3.2 highlights the parameters used for the COMSOL simulations. The surface plots for each particle size are highlighted in Figures 3.7 – 3.9. Similar surface profiles are observed for the three particle sizes. However, bigger particles are difficult to stabilize in pregel solution and will require bigger nozzle sizes also.

Figures 3.10 -3.11 provide visual insight as to how the magnetic field would appear using field lines and surface plots. Figure 3.12 presents the surface plot of magnetic field at a distance of 200 µm from the lower end of the hydrogel with magnetic particles.

Table 3.2: COMSOL Simulation parameters used for obtaining the magnetic field variation

Simulation Parameter	Value
Hydrogel 1 Dimensions	20 µm x 20 µm x 50 µm
Hydrogel 2 Dimensions	20 µm x 20 µm x 50 µm
Number of particles	Determined by weight percentage
Particle location	Distributed uniformly
Particle size	200 nm – 3 µm
Particle magnetization	Size dependent
Physics	Magnetic Field No Current
Meshing type	Free tetrahedral
Minimum size for Meshing	Radius of the magnetic particles
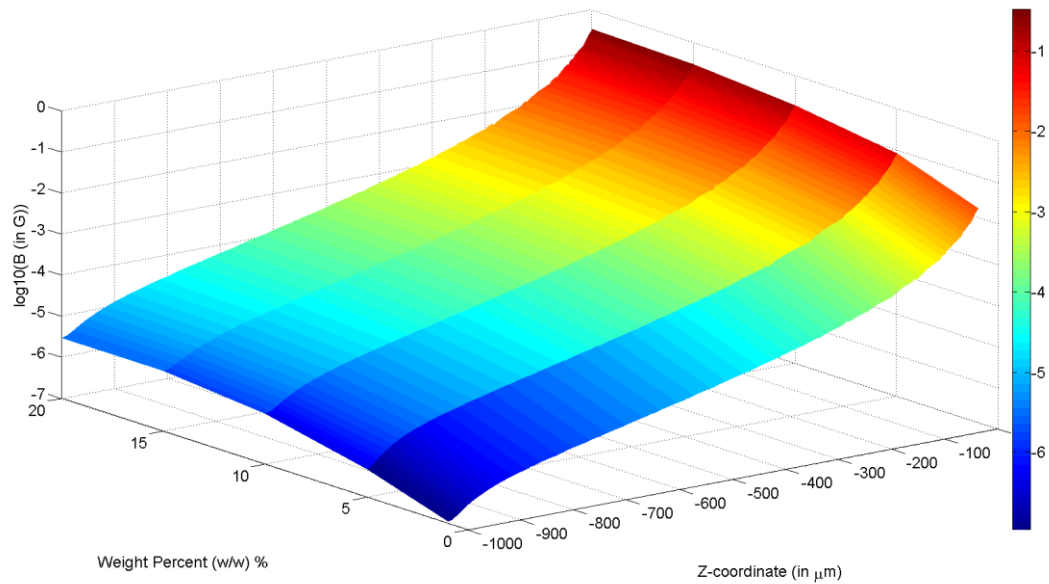
Figure 3.7: Surface plot for magnetic field density variation along the Z-axis at varying particle density for double layered hydrogels with 1 µm magnetic particles in the top layer.
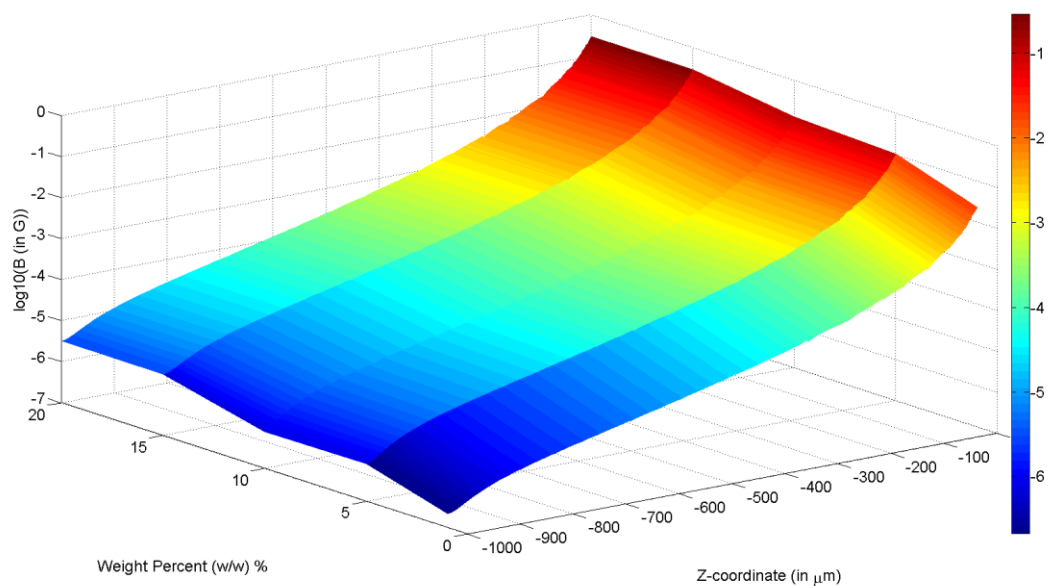
Figure 3.8: Surface plot for magnetic field density variation along the Z-axis at varying particle density for double layered hydrogels with 2 µm magnetic particles in the top layer.
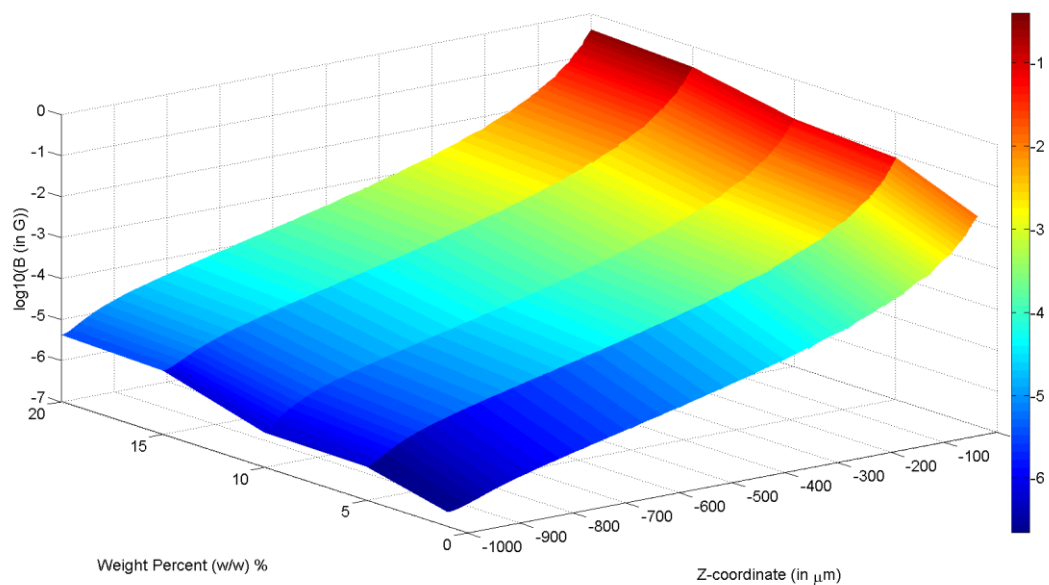
Figure 3.9: Surface plot for magnetic field density variation along the Z-axis at varying particle density for double layered hydrogels with 3 µm magnetic particles in the top layer.

Figure 3.10: Magnetic field visualization in the 3D space (left) and YZ space (right) parallel to the alignment of the magnetic particles inside the hydrogel.

Figure 3.11: Magnetic field visualization in the XY plane perpendicular and XZ parallel to the alignment of the magnetic particles inside the hydrogel.
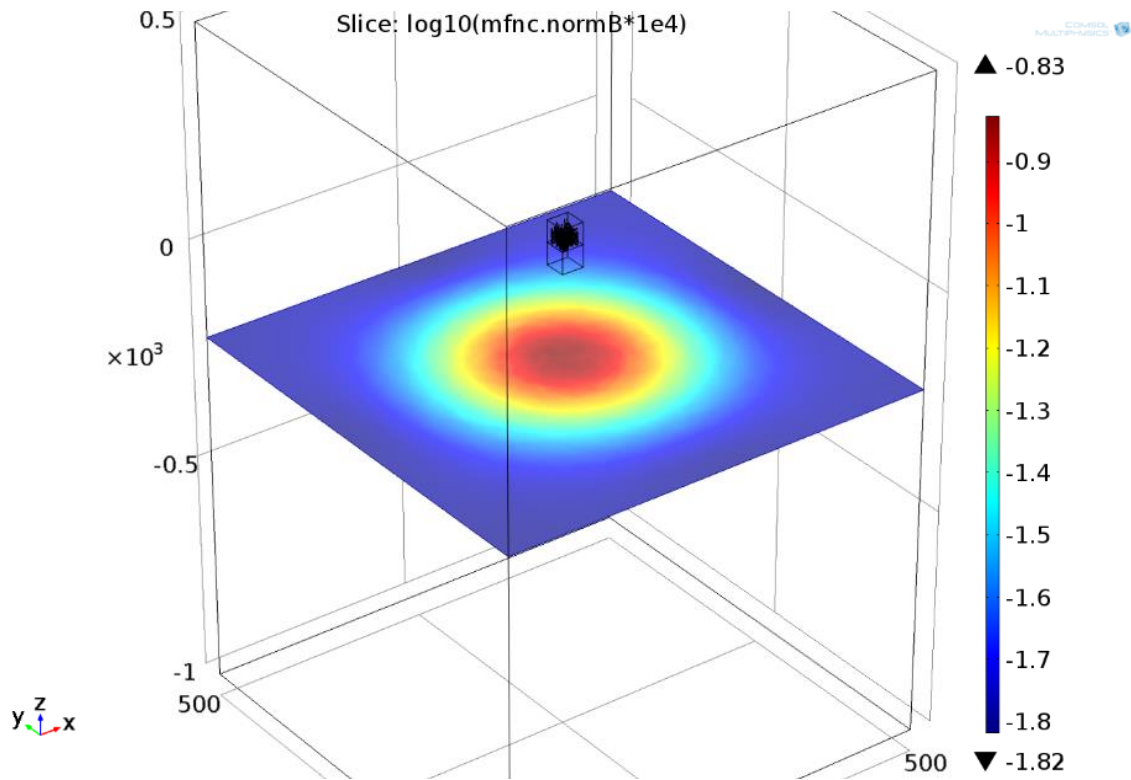
Figure 3.12: Magnetic field perpendicular to the hydrogel in XY plane at a distance of 200 μm from the center.

3.1.5. Magnetic Strip Simulation

COMSOL simulations were performed for the geometry depicted in Figure 3.2, at a remanent magnetization value of 27.9 emu/g, the value obtained for the magnetic sheet of thickness 300 μm.   The results are presented in Figures 3.13-3.15, similar to the visualization results shown for the hydrogel with magnetic particles.

3.2. Pregel Preparation

3.2.1. Composition

The chemical composition used for the pregel solution used for printing glucose sensitive hydrogel was derived from [20] and is shown in Table 3.3.
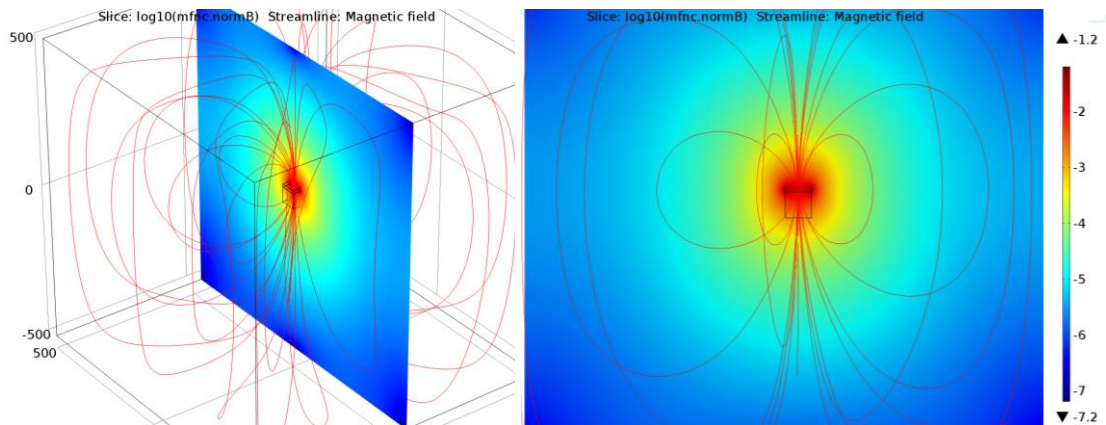
Figure 3.13: Magnetic field visualization in the 3D space (left) and YZ space (right) parallel to the magnetization of the magnetic sheet on top of the hydrogel.
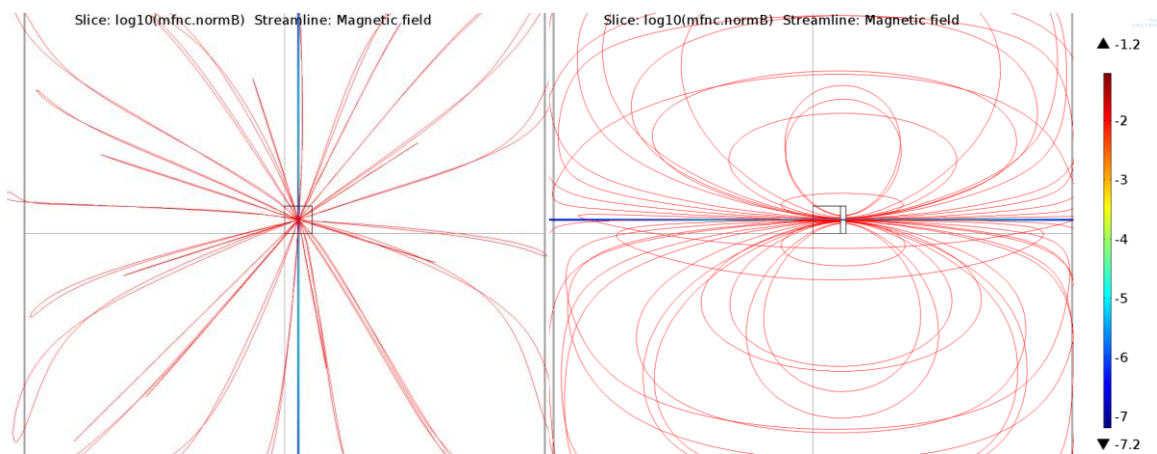
Figure 3.14: Magnetic field visualization in the XY plane perpendicular and XZ parallel to the magnetization of the magnetic sheet on top of the hydrogel.
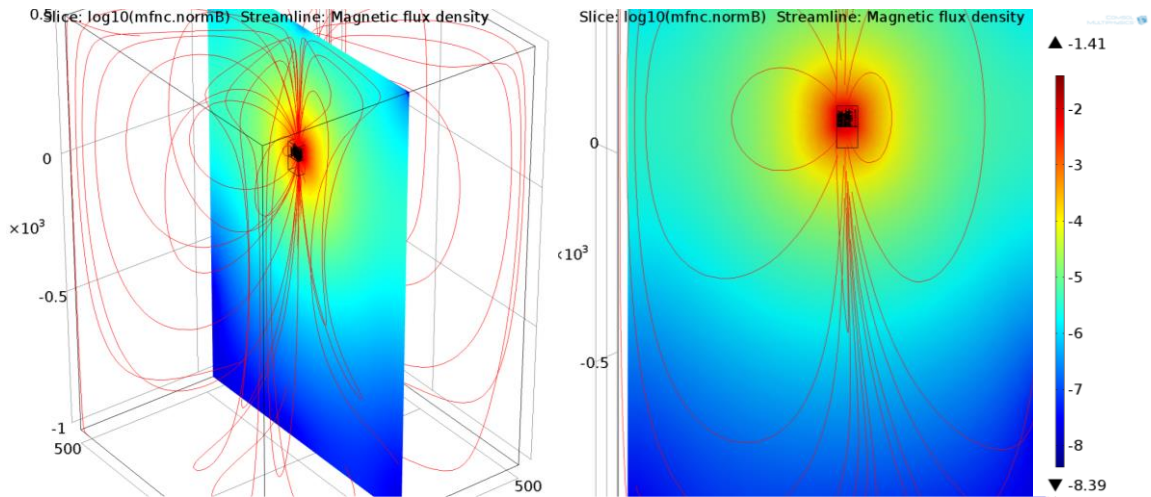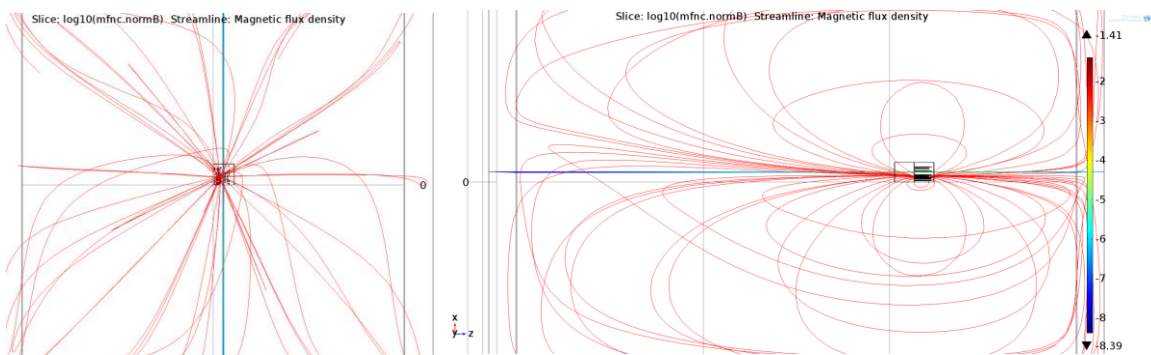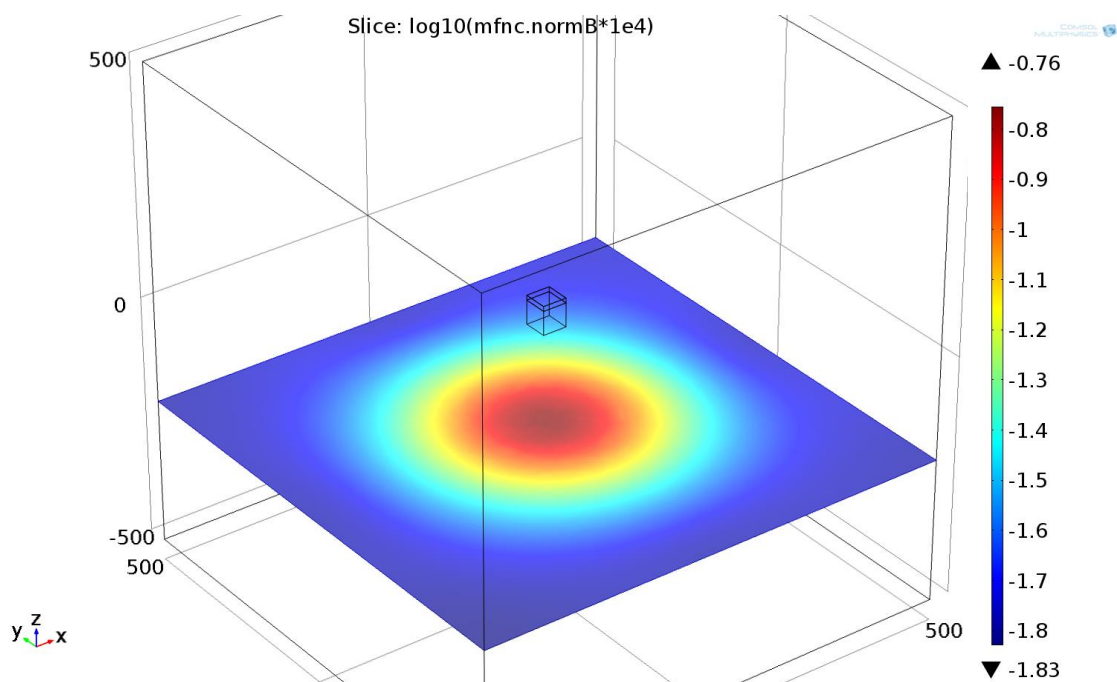
Figure 3.15: Magnetic field perpendicular to the hydrogel in XY plane at a distance of 200 μm from the center.

Table 3.3: Chemical composition of 13 weight % glucose sensitive hydrogel

	Name	molar ratio	Amount (take from stock solution)	stock
1	AAM	80	237 ul	30 wt% in HEPES
2	DMAPAA	10	20.48ul	
3	BIS	2	193ul	2 wt% in HEPES
4	3-APB	8	19.1mg	
5	HEPES buffer		309ul	
6	DMSO		87ul	
7	Initiator mix	v-pyrol/HHMP 10/1	25.8ul	

3.2.2. Magnetic Particle Preparation

One-pot synthesis method as described in [27] was used to produce iron oxide nanoparticles. The method employs thermal decomposition of Fe $(acac)_3$ in 2-pyrrolidone to produce water-soluble iron oxide nano-crystals. These particles were characterized using VSM as described earlier and found to be superparamagnetic.

3.3. Substrate Treatment

As described earlier, substrate treatment plays a crucial role in determining the shape and size of the printed structures as well as to create good physical bonding between the substrate and the printed hydrogel. This section describes the experiments done to determine the effect of oxygen plasma duration on the glass-water contact angle.

3.3.1. Effect of Plasma Duration

Glass cover slips of dimension 22 mm x 2mm and thickness ~0.13-0.17 mm were used for this experiment. These cover slips were cleansed using isopropanol and blow dried. The cover slips were then treated with Dyne-A-Mite™ 3D Treater which uses an air-blown electric arc to form a treatment plasma. Exposure times were varied from 10 seconds to 50 seconds in steps of 10 seconds. Three cover slips were treated for each exposure duration. The contact angle was measured with static sessile drop method using a goniometer. A drop of constant volume was dispensed on the cover slips and the droplet image was recorded using a camera. The setup for capturing the image is shown in Figure 3.16. The images are then analyzed in ImageJ open source software using the contact angle plugin. This plugin requires a selection of five points, two of which define the interface and the
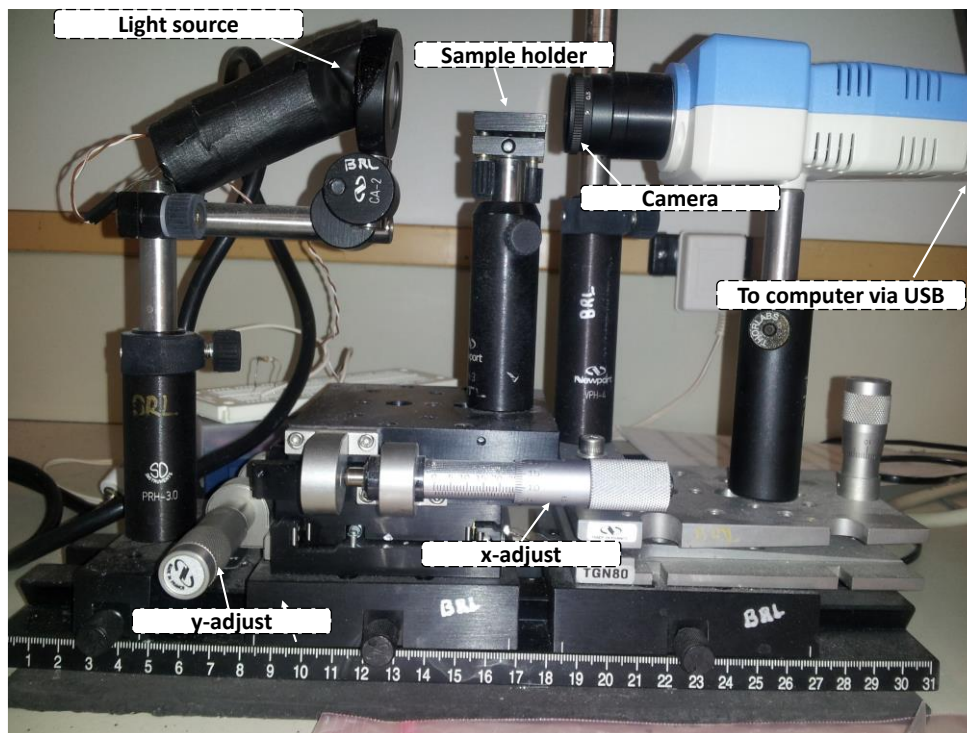
Figure 3.16: Contact angle measurement setup using static sessile drop method. Water droplet is dispensed on the sample placed at the substrate holder, a camera captures the image, which is then transferred via USB to the computer and processed in ImageJ software to compute the contact angle.

other three define the droplet curvature (Figure 3.17). The plugin then computes a best fit as shown in Figure 3.17 and outputs the contact angle. The contact angle was computed this way for all the three samples at each plasma exposure duration and the results are plotted in Figure 3.18.

3.3.2. Height vs. Printed Layers

Inkjet printers dispense ultra-fine ink droplets on the substrate to represent the image or text that is being printed. Because of the extremely high resolutions they offer, they always appear as a continuous print to the naked eyes. However, in the presented application, the ink droplets need to actually meet to form a continuous layer representing
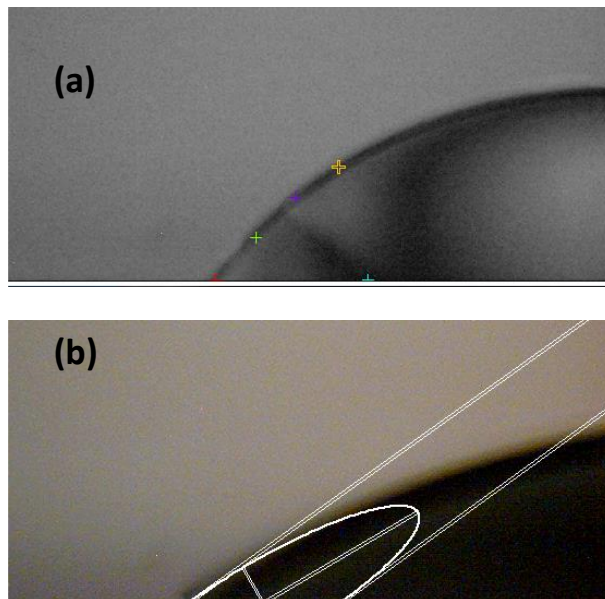
Figure 3.17: Contact angle measurement in ImageJ software using the contact angle plugin. (a) Manual selection of five points to determine the interface and the drop profile (b) the software computes best fit from the points selected and outputs the contact angle.

the printed structure. This experiment basically helped to achieve two tasks: firstly, the minimum number of prints required of the same image to achieve a continuous layer realized on the substrate; secondly, the height of the printed structure versus the number of printed layers, so that the number of prints required can be fed to the printer to achieve the desired hydrogel height.

An Epson Artisan 50 printer was used to print on glass and GelBond® acrylamide film. The minimum number of prints required to produce a continuous layer was found out to be five and four, respectively, for the plasma-treated (duration: 20 seconds) glass and GelBond®. The numbers were higher for untreated glass and polycarbonate surface, which also served as a motivation for plasma activating the glass surface, besides achieving better bonding between the hydrogel and the substrate. The number of layers printed were then varied in steps of five, starting from a minimum of five layers at which the continuous layer
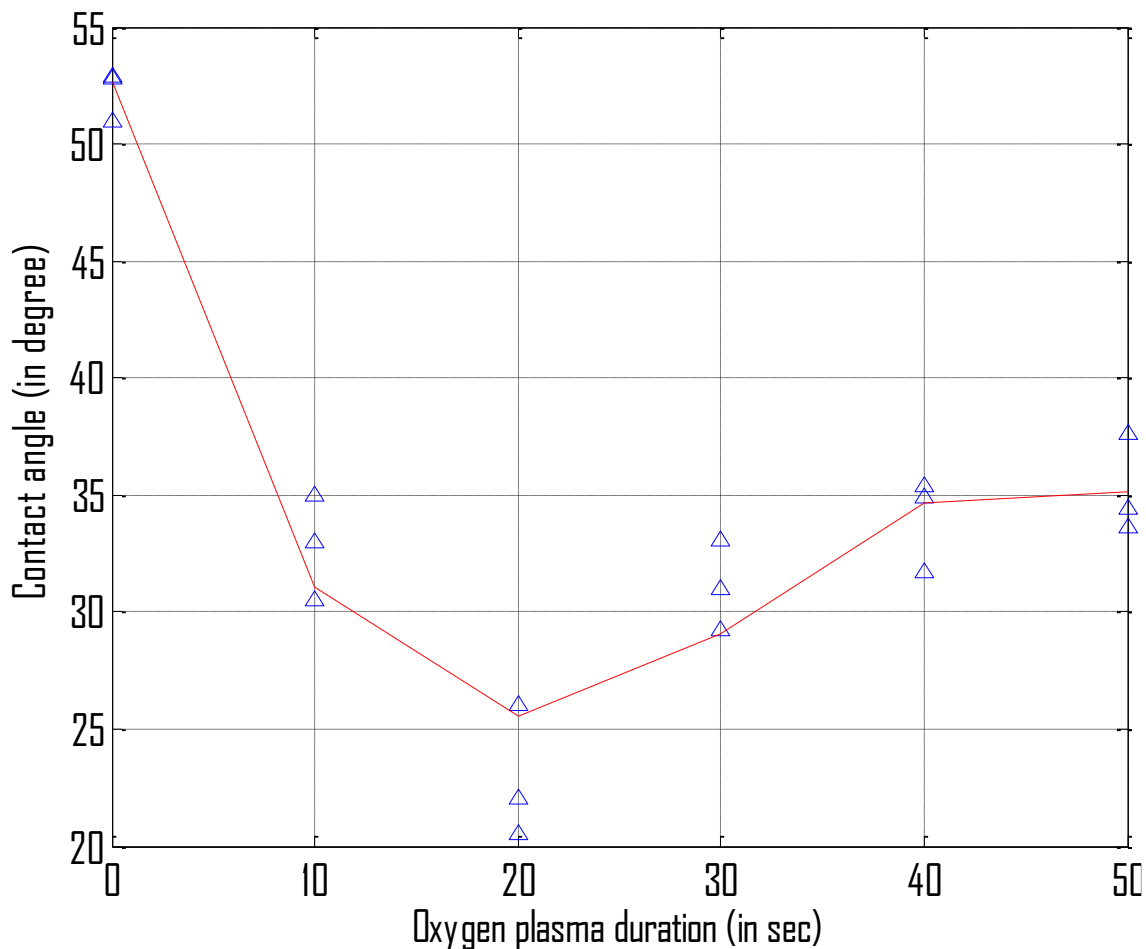
Figure 3.18: Contact angle variation versus oxygen plasma duration. Untreated glass exhibits higher contact angle. The contact angle decreases with increase in plasma duration to a point which is attributed to the appearance of hydroxyl functional groups on the glass surface. The contact angle again increases beyond 30 sec, because of formation of an SiO2 layer that renders the surface hydrophobic.

starts to form. Zygo optical profilometer was used to obtain the surface profiles of these printed structures.

Example Zygo images for the plasma-treated glass substrate and GelBond® substrate are shown in Figure 3.19 and Figure 3.20, respectively. The height of the hydrogels are obtained by selecting lines that span the hydrogel, leveling the glass ends and subtracting from the peak.
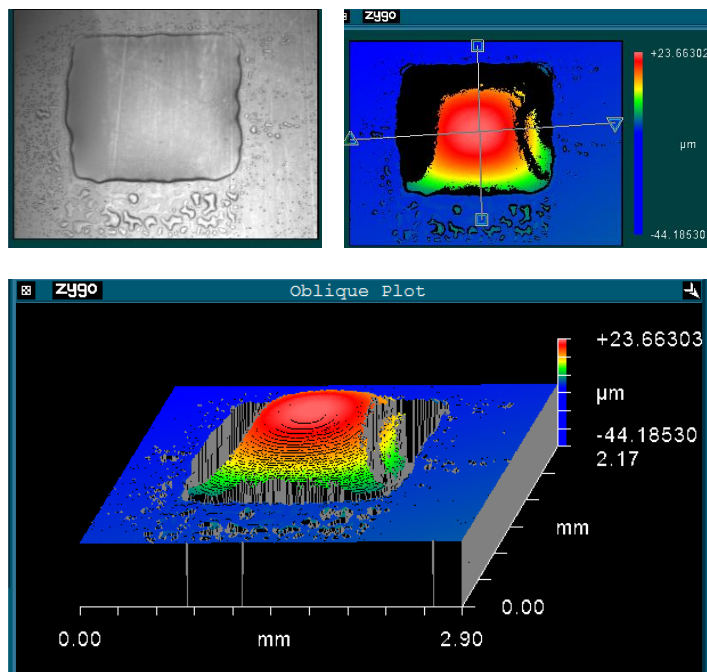
Figure 3.19: Microscope image and surface profile of hydrogel printed on plasma-treated glass substrate. The height at the center of the hydrogel is computed by doing curve leveling.
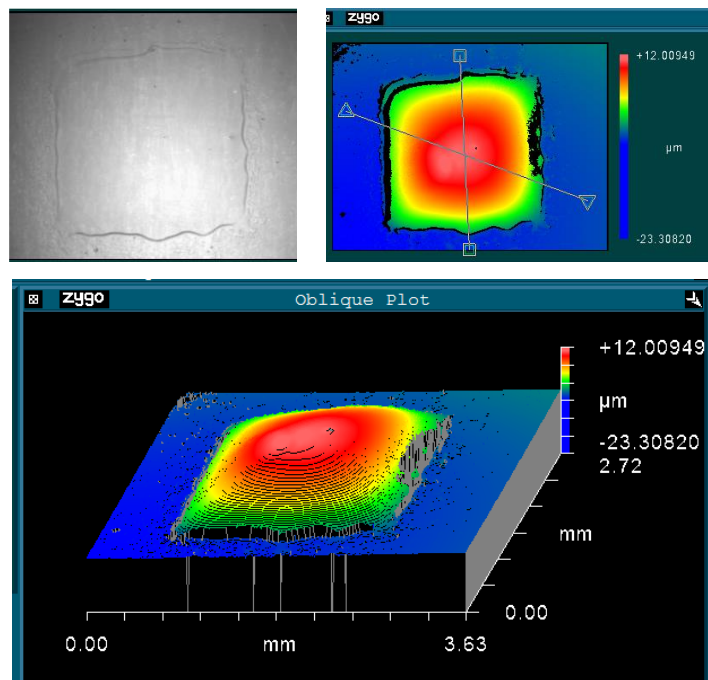
Figure 3.20: Microscope image and surface profile of hydrogel printed on GelBond® substrate. The height at the center of the hydrogel is computed by doing curve leveling.

For each number of printed layers, multiple samples were printed to obtain the average height of these printed structures. Results for the height of the printed hydrogels versus the number of layers printed are shown in Figure 3.21 and 3.22 for the plasma-treated glass substrate and GelBond® film, respectively. It is observed that the height of printed structures increases linearly with the number of printed layers.

3.3.3. Printing of Hydrogel with Magnetic Particles

We were able to dispense the pregel solution with the in-house synthesized magnetic particles. However, because the particles were found to be superparamagnetic, the composite gels with embedded magnetic particles were not characterized for their response time. 1 µm Strontium ferrite particles were used instead because of their high remanent
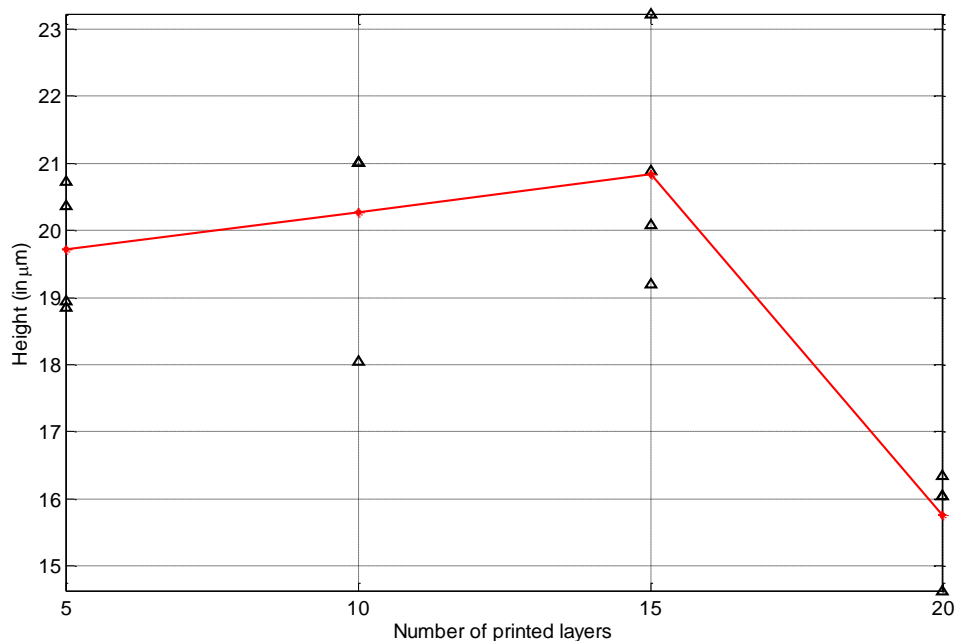
Figure 3.21: Height of the printed hydrogels on plasma (20 seconds) treated glass substrate versus the number of layers printed. There is a linear increase in the height of the printed structure with number of layers.
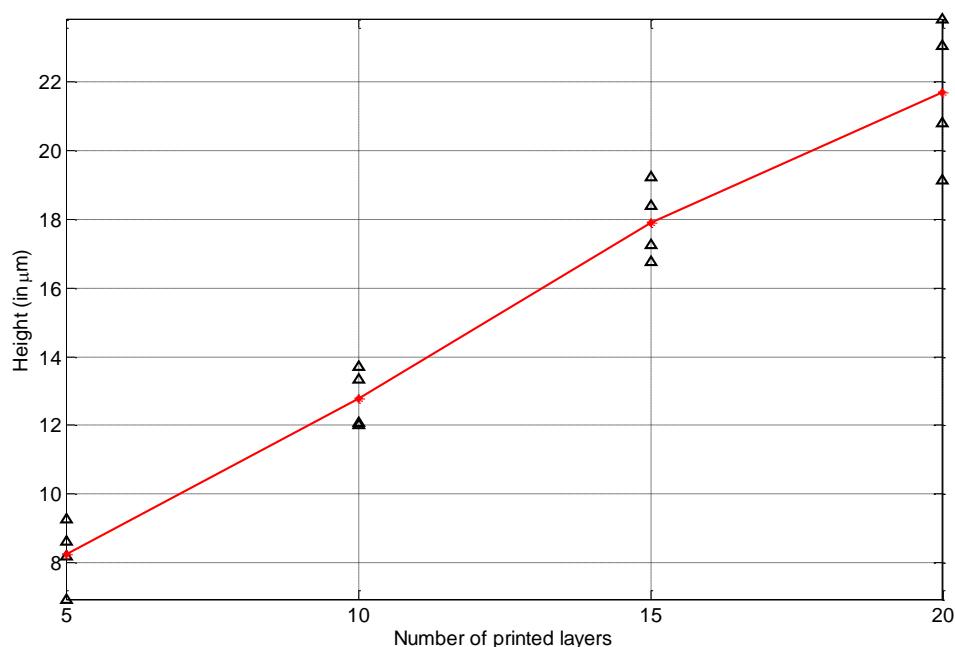
Figure 3.22: Height of the printed hydrogels on GelBond® versus the number of layers printed. There is a linear increase in the height of the printed structure with number of layers printed.

magnetization. However, these particles could neither be stabilized inside pregel solution nor could they be dispensed through the printer. Hence, the hydrogel samples for characterization were prepared manually. Their preparation is discussed in detail in following sections.

3.4. Hydrogel Characterization

3.4.1. Setup Design

Figure 3.23 presents the setup used for characterizing the hydrogels' response to variation in the concentration of analytes. A Honeywell 3-Axis Digital Compass IC HMC5883L was used to detect the variation in the magnetic field induced by the swelling/de-swelling of the hydrogel. This magnetometer transmits the data via Zigbee RF
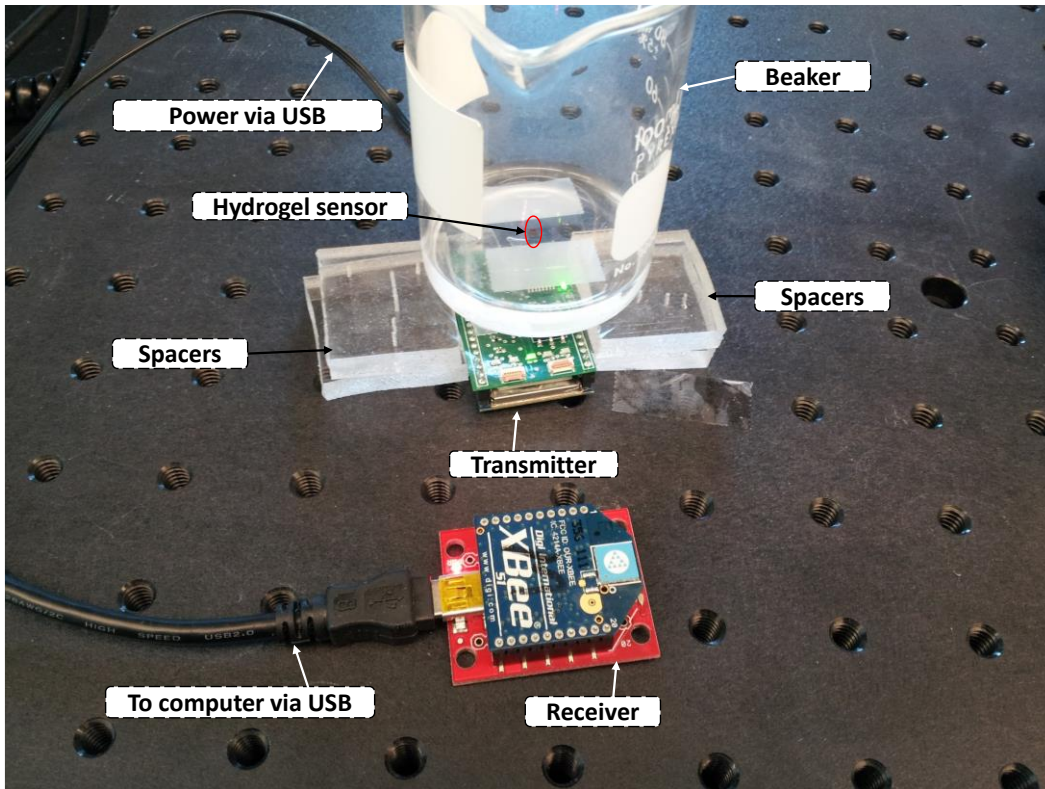
Figure 3.23: Experimental setup used for characterizing hydrogel's response. The 3-axis Honeywell magnetometer detects the change in magnetic field on swelling/deswelling of the hydrogel in response to the variation in the analytes. The output of the magnetometer is transmitted via ZigBee RF link to the computer where the response is displayed.

link (Figure 3.24) to the receiver which interfaces with the computer via USB. Both the transmitter and receiver are powered through the USB port from the computer. The measuring range on the magnetometer is limited. Therefore, a set of spacers are used to maintain the required spacing from the hydrogel to the magnetometer such that it does not saturate the magnetometer reading. The readings from the magnetometer are read at intervals of 0.5 seconds and displayed real time using MATLAB. The plotting window is set to automatic range type and controls the display axis. The X, Y, and Z components along with the total magnitude of the read magnetic field are displayed in four different subplots.
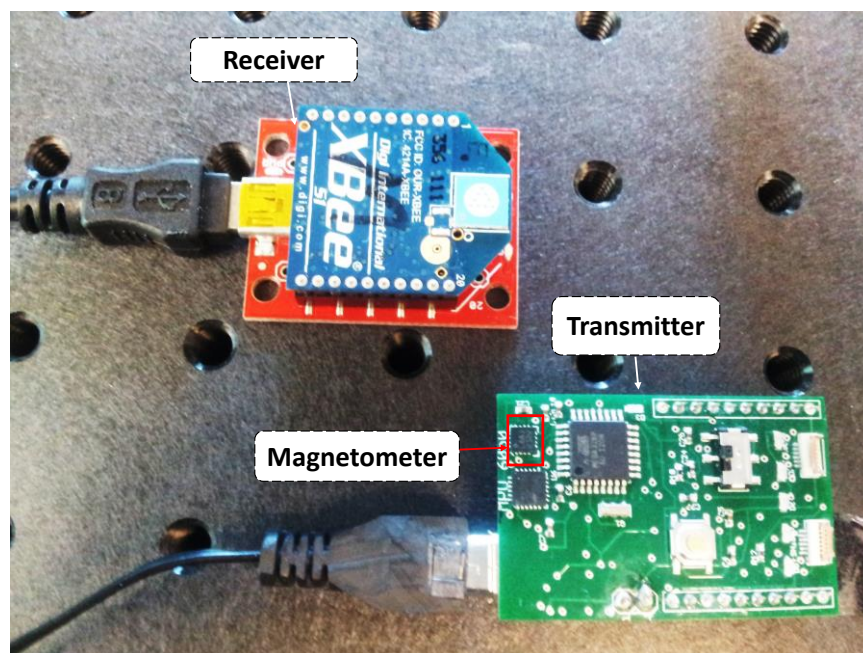
Figure 3.24: Zigbee embedded RF module for transmitting and receiving the magnetometer signal.

3.4.1. Hydrogel with Magnetic Strip

The first set of characterization experiments was performed with the hydrogel with magnetic sheets on the top. These sheets were magnetized as described earlier using the VSM and carry a remanent magnetization of 27.9 emu/g and 22.4 emu/g, respectively, for thickness 300 μm and 230 μm. These sheets roughly 5 mm x 5 mm in shape were further cut into six smaller parts. Pregel solution is dispensed on plasma-treated (duration = 20 s) 22 mm x 22 mm square glass cover slips. Spacers are used to control pregel solution height to 100 μm and squeezing out any extra solution.

The dispensed pregel solution is exposed to UV light for 15 seconds to partially polymerize it. This is done to ensure bond formation between the first and second layer of the hydrogels, when polymerizing the latter. The magnetic sheet is then laid on top of this partially polymerized layer. Pregel solution is then dispensed on top of this magnetic sheet

using enough spacers to cover the sheet completely. The composite structure is exposed to UV again for about 20 seconds to ensure complete polymerization of the layers. The second hydrogel layer covering the magnetic strip protects the magnetic strip from dislodging from the hydrogel when placed in the solution. The process of synthesizing the hydrogels with magnetic sheet is depicted in Figure 3.25.

After conditioning the prepared hydrogel, the cover slip was secured at the bottom of beaker using scotch tape. Next, the hydrogel's response was obtained for varying ionic strength of the PBS solution in the beaker repeatedly between 1X and 0.5X. The time intervals are set to allow sufficient time for the sensor to settle down to the steady state values. As the concentration of the solution increases, the hydrogel shrinks, which implies a lower distance of the magnetic strip from the magnetometer and hence a stronger

Figure 3.25: Synthesis process for hydrogel with magnetic sheet on top. Spacers are used to control the thickness of lower hydrogel. The magnetic sheet is laid on top of the lower hydrogel and covered using pregel solution and polymerized to generate the intended structure.

magnetic field. This is evident from the characterization results shown in Figure 3.26. A linear drift was observed with time in the sensor's response and was compensated by doing a simple de-trending operation in MATLAB. Both the original and drift compensated responses are shown in Figure 3.26.

Further, the time constants τ_{90} and τ_{60} were computed to determine the sensor's response time. τ_{90} and τ_{60} are determined as the time taken for the sensor to reach 90% and 60% of the difference between the initial and final steady values. The average values for τ_{90} and τ_{60} were computed to be 5.78 minutes and 2.57 minutes, respectively.

Figure 3.26: Characterization results for hydrogel with magnetic sheet on top for varying ionic strength

3.4.2. Double Hydrogel with Magnetic Particles

The first layer is synthesized the same way as described in the previous section using spacers on plasma-treated glass cover slips as the substrate. Strontium ferrite magnetic particles of size 1 μm were magnetized to their saturation values by applying a magnetic field of 0.8 T and mixed in the pregel solution 5% by weight. After partially polymerizing the first layer for 10 s, the pregel solution with magnetic particles was dispensed on top. The particles were aligned vertically inside the pregel solution using a bar magnet. The composite structure was then polymerized using UV light for about 15 sec. The total duration is reduced from previous synthesis to avoid excessive hardening of the synthesized hydrogels, because here, the first layer is not blocked as in the case of using a magnetic strip. The synthesis steps are outlined in Figure 3.27.

The hydrogel was conditioned and characterized in a similar fashion as the previous section by varying the concentration repeatedly between 1X and 0.5 X. The original and drift compensated results are shown in Figure 3.28. The average values for τ_{90} and τ_{60} for this sensor were computed to be 15.9 minutes and 10.2 minutes, respectively.

3.4.3. Magnetometer Characterization

Magnetometer characterization is needed to translate the variations in its response to the swelling or de-swelling of the hydrogel sensors. Varying magnetic field strength recorded by the magnetometer versus the distance from the magnetic source can be used as a look-up table to calibrate the hydrogel sensor's response for varying ionic strength. For this, a linear actuator system was assembled to vary the distance of magnet source from the hydrogel with the magnetic sheet or particles on top in a cyclic fashion.
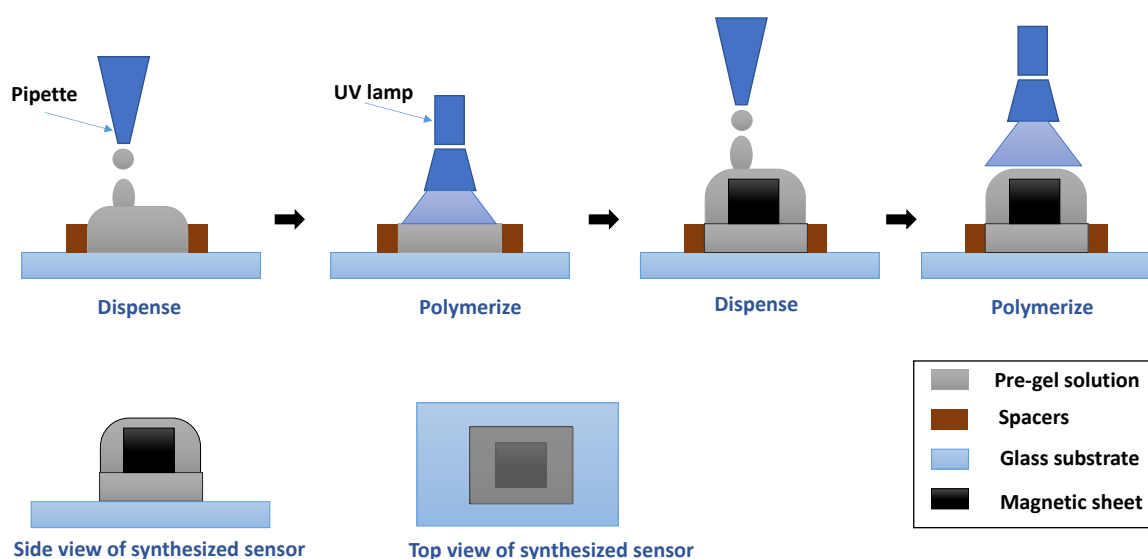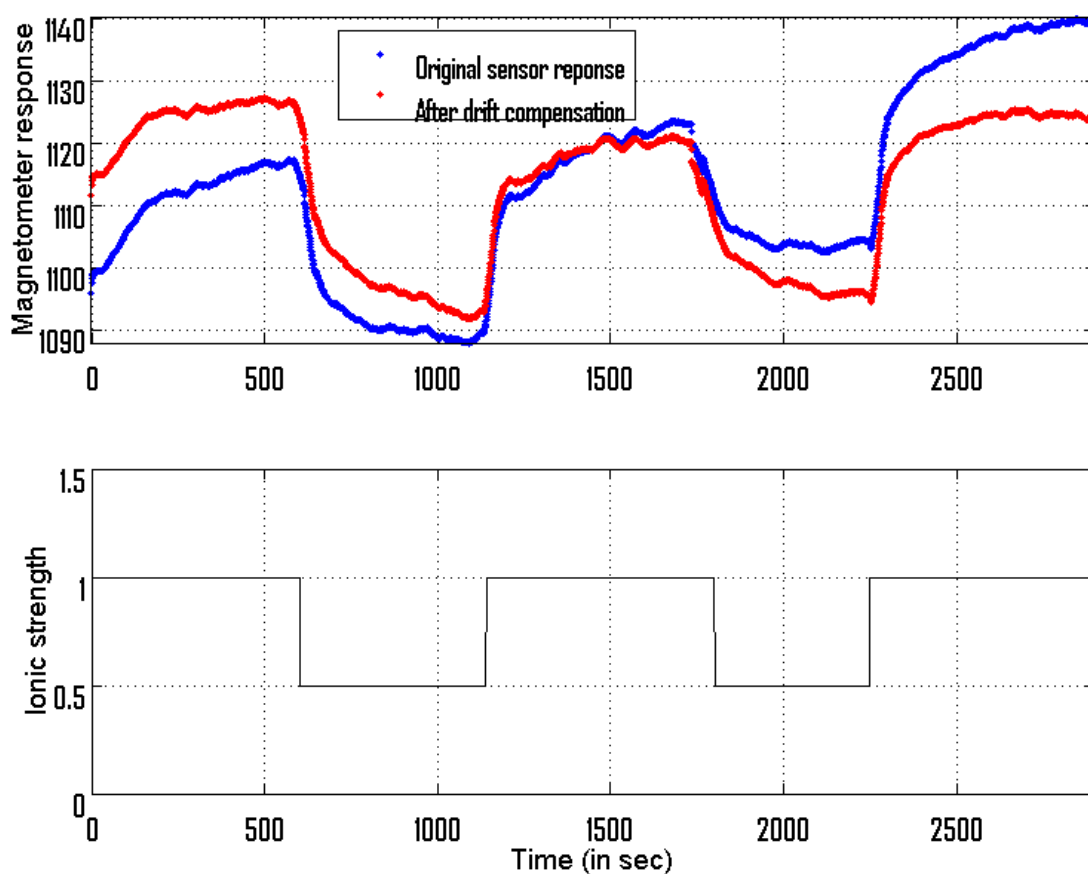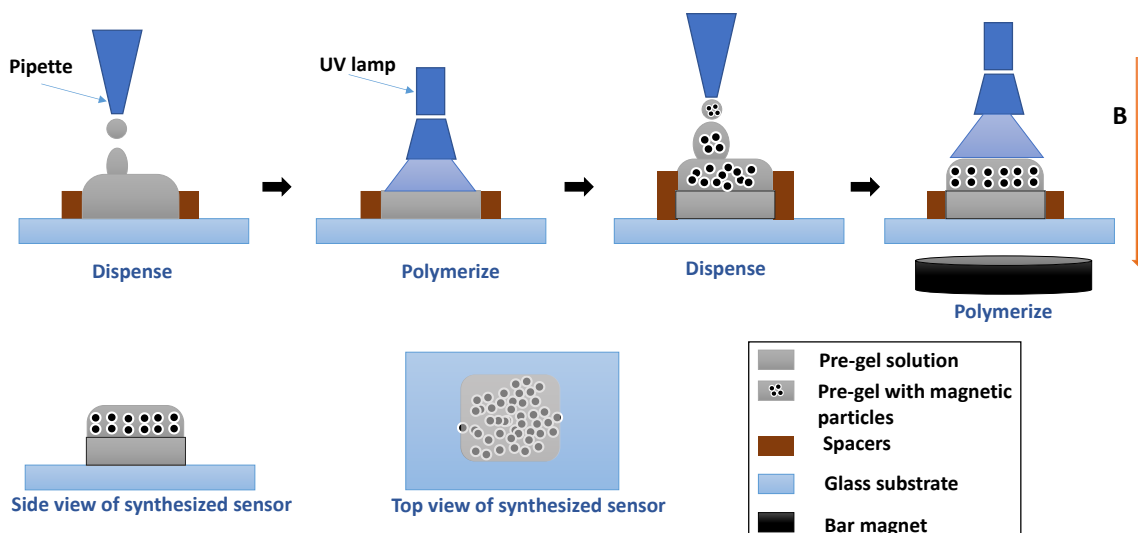
Figure 3.27: Synthesis process for hydrogel with magnetic sheet on top. Spacers are used to control the thickness of lower hydrogel. The pregel with magnetic particles is laid on top of the lower hydrogel and polymerized in presence of external magnetic field to generate the intended structure.
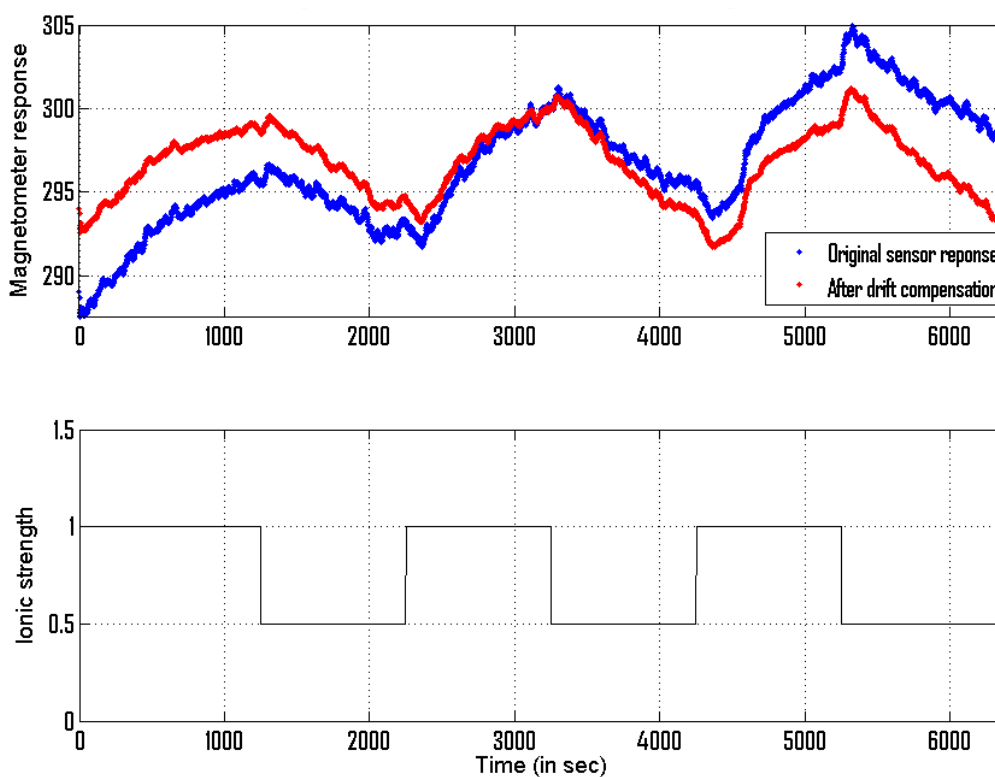
Figure 3.28: Characterization results for double layered hydrogel for varying ionic strength. The results are for 5 % w/w magnetic particles in the top layer of the hydrogel.

The transmitter and receiver were connected as described earlier via the USB port to computer. The linear actuator is also interfaced via the USB and its movement is controlled through MATLAB. For each displacement of the linear actuator, six readings are taken at an interval of 0.5 seconds and averaged out to reduce the noise in the readings. The linear actuator is moved in both the directions, such that two readings can be taken at each displacement in either direction. These values for a displacement of 7.5 mm in steps of 500 nm in each direction are shown in Figure 3.29.

Figure 3.29: Magnetometer characterization by varying height of the magnetic sheet from the magnetometer. Inverse cubic response is observed as expected.

4. CONCLUSIONS AND FUTURE WORK

This project presented a process that employs inkjet printing to synthesize accurate hydrogel structures. An Epson Artisan 50 inkjet printer was used to dispense pregel solution to synthesize hydrogel structures of varying shapes and sizes. The printer could also print composite hydrogels with embedded nanoparticles that were synthes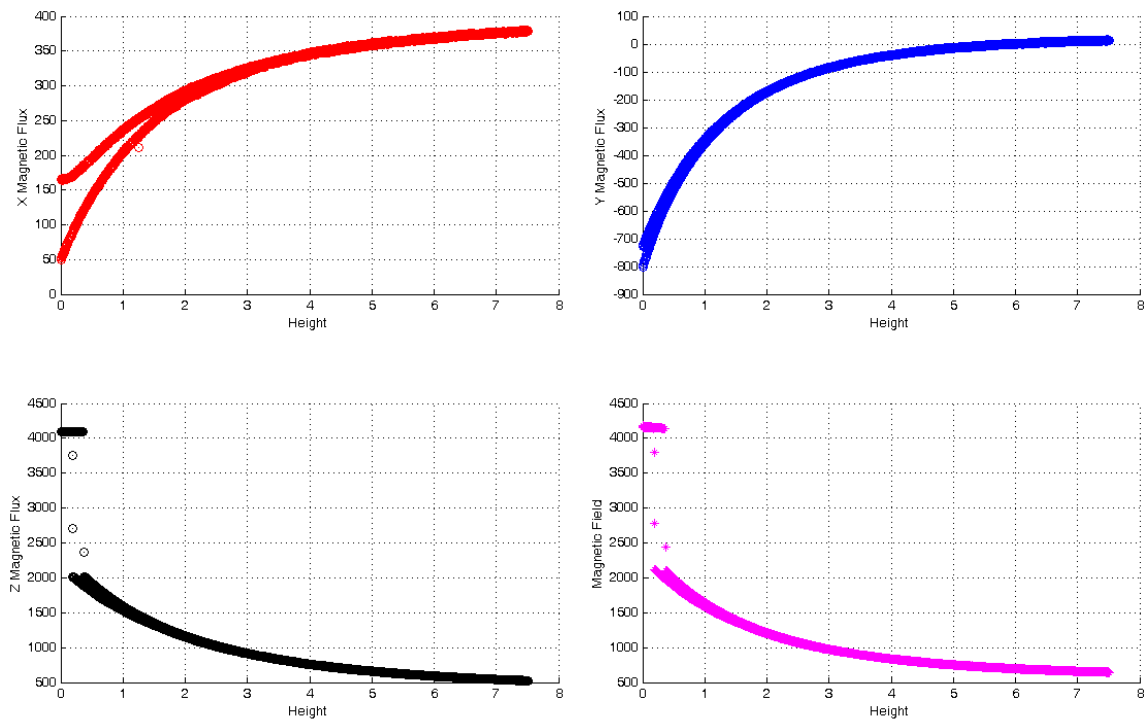ized in house. However, the nozzle size and particle agglomeration issues were encountered when dispensing pregel with embedded strontium ferrite microparticles.

Substrate treatment was explored to improve the shape and spread of the printed structures. Oxygen plasma treatment was used to activate glass surface. It was observed that plasma not only lowered the contact angle, it also enables the formation of a weak physical bond between the hydrogel and glass substrate. The use of GelBond® acrylamide film is also a potential option because it offers better spread without the need of any surface treatment. However, its use is limited to acrylamide-based hydrogels only.

A set of COMSOL simulations was performed that provided insights into the magnetic field strength variation for the intended hydrogel structures. The results were presented as 3D surface plots and magnetic field lines for better visualization and guidelines for characterization experiments.

The in-house synthesized magnetic particles were characterized using VSM and were found to be superparamagnetic. Therefore, for characterization experiments, the magnetic

hydrogel composites were synthesized manually using spacers to control the thickness. Two types of magnetic hydrogel composites were synthesized, one with magnetic sheet on top of hydrogel and the other with magnetic particles embedded and aligned vertically inside the hydrogel. These were characterized to have response times (τ_{90}) of 6 minutes and 15 minutes, respectively, for changes in ionic strength of Phosphate buffered saline (PBS) from 0.5x to 1x.

Inkjet printing is a great solution for synthesizing accurate and fast hydrogel-based smart sensors and offers the potential for an inexpensive commercial-scale synthesis method. With the right nozzle size, it should be feasible to dispense pregel with particle sizes ranging in microns, provided they can be stabilized inside the pregel solution.

4.1. Future Work

1. Explore the use of magnetometers with higher sensitivity to obtain better signal to noise ratio when dealing with magnetic hydrogels with embedded magnetic particles.

2. Investigate printheads that allow easy dispensing of the pregel solution with dispersed magnetic particles with sizes up to a few microns.

3. Automate the process of printing and polymerization by controlling the printhead and UV light source through a single controller.

4. Explore more techniques for alignment of the particles to achieve the best signal transduction for hydrogel swelling and deswelling in response to environment changes.

REFERENCES

[1] N. Sahiner, "Soft and flexible hydrogel templates of different sizes and various functionalities for metal nanoparticle preparation and their use in catalysis," *Progress in Polymer Science*, vol. 38, no. 9, pp. 1329–1356, Sep. 2013.

[2] S. Dwivedi, "Hydrogel-A Conceptual Overview," *International Journal of Pharmaceutical & Biological ...*, vol. 2, no. 6, pp. 1588–1597, 2011.

[3] S. R. Raghavan and J. F. Douglas, "The conundrum of gel formation by molecular nanofibers, wormlike micelles, and filamentous proteins: gelation without cross-links," *Soft Matter*, vol. 8, no. 33, p. 8539, 2012.

[4] A. S. Hoffman, "Hydrogels for biomedical applications.," Annals of the New York Academy of Sciences, vol. 944, pp. 62–73, Dec. 2001.

[5] A. Gibas and H. Janik, "Review : Synthetic Polymer Hydrogels for Biomedical," Chemical Technology, vol. 4, no. 4, pp. 297–304, 2010.

[6] K. Park, W. Shalaby and H. Park, *Biodegradable hydrogels for drug delivery*. Lancaster, PA: Technomic Pub., 1993.

[7] B. Ratner and A. Hoffman, "Synthetic hydrogels for biomedical applications," *Hydrogels for Medical and Related Applications, ACS Symposium Series*, vol. 31, pp. 1-36, 1976.

[8] J. Bates, "pH-responsive hydrogel-based chemomechanical sensors designed for disposable bioreactor applications," PhD Dissertation, Department of Materials Science and Engineering, The University of Utah, Salt Lake City, UT, 2013.

[9] E. Tekin, P. J. Smith, and U. S. Schubert, "Inkjet printing as a deposition and patterning tool for polymers and inorganic particles," *Soft Matter*, vol. 4, no. 4, pp. 703–713, 2008.

[10] P. Calvert, "Inkjet Printing for Materials and Devices," *Chemistry of Materials*, vol. 13, no. 10, pp. 3299–3305, Sep. 2001.

[11] A. Kamyshny, "Metal-based inkjet inks for printed electronics," *Open Applied Physics Journal*, vol. 4, no.1 1, pp. 19–36, 2011.

[12] A. Hudd, "Inkjet printing technologies," *The Chemistry of Inkjet Inks. New Jersey: World Scientific*, pp. 3–18, 2010.

[13] D. McCallum, C. Ferris, P. Calvert, G. Wallace, and M. in het Panhuis, "Printed hydrogel materials," *ICONN 2010, International Conference on Nanoscience and Nanotechnology*. pp. 257–260, 2010.

[14] Y. Nishiyama, M. Nakamura, C. Henmi, K. Yamaguchi, S. Mochizuki, H. Nakagawa, and K. Takiura, "Development of a Three-Dimensional Bioprinter: Construction of Cell Supporting Structures Using Hydrogel and State-Of-The-Art Inkjet Technology," *Journal of Biomechanical Engineering*, vol. 131, no. 3, p. 35001, Dec. 2008.

[15] R. Zhang, A. Liberski, F. Khan, J. J. Diaz-Mochon, and M. Bradley, "Inkjet fabrication of hydrogel microarrays using in situ nanolitre-scale polymerisation," *Chem. Commun.*, no. 11, pp. 1317–1319, 2008.

[16] S. Limem, D. McCallum, G. Wallace, and P. Calvert, "Inkjet printing of self-assembling polyelectrolyte hydrogels," *Soft Matter*, vol. 7, pp. 3818–3826, 2011.

[17] K. J. Nossent, "Using inkjet technology to deposit functional materials", Oral Presentation, *SGIA Printed Electronics Conference*, 2011.

[18] I. S. Han, M.-H. Han, J. Kim, S. Lew, Y. J. Lee, F. Horkay, and J. J. Magda, "Constant-Volume Hydrogel Osmometer: A New Device Concept for Miniature Biosensors," *Biomacromolecules*, vol. 3, no. 6, pp. 1271–1275, 2002.

[19] D.-Y. Jung, J. J. Magda, and I. S. Han, "Catalase Effects on Glucose-Sensitive Hydrogels," *Macromolecules*, vol. 33, no. 9, pp. 3332–3336, Apr. 2000.

[20] G. Lin, S. Chang, H. Hao, P. Tathireddy, M. Orthner, J. Magda, and F. Solzbacher, "Osmotic swelling pressure response of smart hydrogels suitable for chronically implantable glucose sensors," *Sensors and Actuators B: Chemical*, vol. 144, no. 1, pp. 332–336, 2010.

[21] O. Philippova, A. Barabanova, V. Molchanov, and A. Khokhlov, "Magnetic polymer beads: Recent trends and developments in synthetic design and applications," *European Polymer Journal*, vol. 47, no. 4, pp. 542–559, 2011.

[22] F. D. Egitto and L. J. Matienzo, "Plasma modification of polymer surfaces for adhesion improvement," *IBM Journal of Research and Development*, vol. 38, no. 4. pp. 423–439, 1994.

[23] M.White, "The removal of die bond/epoxy bleed material by oxygen plasma", *Proceedings 32nd IEEE Electronic Components Conference*, pp. 262, 1982.

[24] S. Bhattacharya, a. Datta, J. M. Berg, and S. Gangopadhyay, "Studies on surface wettability of poly(dimethyl) siloxane (PDMS) and glass under oxygen-plasma treatment and correlation with bond strength," *Journal of Microelectromechanical Systems*, vol. 14, no. 3, pp. 590–597, Jun. 2005.

[25] K.-B. Lim and D.-C. Lee, "Surface modification of glass and glass fibres by plasma surface treatment," *Surface and Interface Analysis*, vol. 36, no. 3, pp. 254–258, Mar. 2004.

[26] A. V Smirnov, "Grain size dependence of low-temperature remanent magnetization in natural and synthetic magnetite : Experimental study," pp. 119–124, 2009.

[27] W. M. Nanocrystals, "One-Pot Reaction to Synthesize Water-Soluble Magnetite Nanocrystals," vol. 16, no. 8, pp. 12–14, 2004.